

**FOR REFERENCE**

**NOT TO BE TAKEN FROM THIS ROOM**

---

# **Comparison of Calculated and Measured Pressures on Straight- and Swept-Tip Model Rotor Blades**

---

Michael E. Tauber, I-Chung Chang, David A. Caughey  
and Jean-Jacques Philippe

---

December 1983

**LIBRARY COPY**

FEB 6 1984

LANGLEY RESEARCH CENTER  
LIBRARY, NASA  
HAMPTON, VIRGINIA



National Aeronautics and  
Space Administration

3 1176 00517 7812

---

# Comparison of Calculated and Measured Pressures on Straight- and Swept-Tip Model Rotor Blades

---

Michael E. Tauber,  
I-Chung Chang, Ames Research Center, Moffett Field, California  
David A. Caughey, Cornell University, Ithaca, New York  
Jean-Jacques Philippe, ONERA, Chatillon, France



National Aeronautics and  
Space Administration

**Ames Research Center**  
Moffett Field, California 94035

N/84-16143#



# COMPARISON OF CALCULATED AND MEASURED PRESSURES ON STRAIGHT- AND SWEPT-TIP MODEL ROTOR BLADES

Michael E. Tauber, I-Chung Chang, David A. Caughey,\*  
and Jean-Jacques Philippe†

Ames Research Center

## SUMMARY

Using the quasi-steady, full potential code, ROT22, pressures were calculated on straight- and swept-tip model helicopter rotor blades at advance ratios of 0.40 and 0.45, and into the transonic tip speed range. The calculated pressures were compared with values measured in the tip regions of the model blades. Good agreement was found over a wide range of azimuth angles when the shocks on the blade were not too strong. However, strong shocks persisted longer than predicted by ROT22 when the blade was in the second quadrant. Since the unsteady flow effects present at high advance ratios primarily affect shock waves, the underprediction of shock strengths is attributed to the simplifying, quasi-steady, assumption made in ROT22.

## INTRODUCTION

The emphasis on increasing helicopter flight speed has resulted in higher rotor advance ratios and tip Mach numbers. However, it is essential that desired performance improvements not be made at the expense of increasing noise. The formation of shock waves in the transonic flow on the advancing blade is a major source of high power requirement and high-speed noise. Therefore, it is essential to understand and to calculate this three-dimensional, unsteady, transonic flow field.

The first three-dimensional, transonic calculations for flow over rotor blades were performed by Caradonna and Isom (ref. 1), using small disturbance theory. The calculations were made for a nonlifting rotor in hover such that the tip speed was representative of forward flight. Subsequently, this steady formulation was extended to the unsteady, forward flight case (ref. 2); however, the spanwise free-stream velocity component due to rotation was assumed to be small and thus ignored. Grant (ref. 3) included all free-stream velocity components in his solution of the transonic small disturbance equation for nonlifting forward flight, but assumed quasi-steady flow.

In contrast to the difficulties encountered in calculating the rotary wing flow field, computer codes for solving the three-dimensional transonic flow over lifting fixed wings have been available for some time. A widely used one is the full potential code, FLO22, developed by Jameson and Caughey (ref. 4). The FLO22 code solves the nonconservative, inviscid, full potential equation using exact surface tangency boundary conditions. The ROT22 code (refs. 5 and 6) was developed by reformulating FLO22 to calculate the flow about a lifting rotor blade in forward flight. Although the full potential equation is solved, the formulation is quasi-steady in that the time derivatives of the perturbation potentials were neglected in the interest of

---

\*Cornell University, Ithaca, New York.

†ONERA, Chatillon, France.

greatly speeding the computation. Since the unsteadiness of the flow increases with advance ratio, it is important to determine the effect of the quasi-steady assumption on the flow field calculation at high advance ratios. Also in high-speed forward flight, it was proven advantageous to sweep the blade tips to delay shock formation. The objective of the present computation/experiment comparison is to determine the ability of the ROT22 code to predict pressure distributions on non-lifting straight- and swept-tip blades at high rotor speeds and high advance ratios.

## TEST CONDITIONS AND MODEL CONFIGURATIONS

The pressure measurements used were made by ONERA (refs. 7 and 8) on modified Alouette helicopter tail rotor models having nonlifting, symmetrical, airfoil sections. The test was conducted using a rotor on a stand in a wind tunnel; rotor speed and tunnel velocities were varied to achieve desired advance ratios. Two different rotor blade configurations were tested. One had a nearly straight leading edge and a 75-cm radius from the center of rotation (fig. 1); the second configuration (which had a radius of 83.5 cm) had 30° of leading edge sweep on the outer 15% (fig. 2). Both types of blades had symmetric NACA four-digit airfoils, varying in thickness-to-chord ratio from 17% at the widest chord station to 9% at the tip.

Instrumentation on both blades consisted of three chordwise rows of Kulite LDQL pressure transducers, nominally at the 85%, 90%, and 95% radial stations. To achieve the desired instrumentation density, two tips were built for each configuration. The straight tips were nearly identical. However, the swept tips differed slightly, thus introducing some scatter in the data, notably at the middle, most densely instrumented, stations. The measured data were transmitted via an electro-pneumatic switch and slip rings to amplifiers. Mean instantaneous pressures were computer averaged; values were measured at 256 blade azimuthal positions. On the straight blade, the thickness-to-chord ratios at the instrumented stations were, in the direction of the tip, 13.1%, 12.15%, and 10.6%; while for the swept-tip blade the ratios were 13.5%, 12%, and 10.5%.

## COMPUTATIONS

The ROT22 code, described in references 5 and 6, with the correction of reference 9, was used to calculate the pressure distributions on the blades. ROT22 solves a quasi-steady approximation to the three-dimensional, full potential equation in a blade-attached coordinate system. The quasi-steady approximation greatly reduces computation time, since the true time-dependent history of the solution need not be computed. A computational grid of 120 points chordwise, 16 vertically, and 24 spanwise, was used for the straight blade; resolution was more critical for the swept-tip blade, and the number of spanwise stations was increased to 32. About two-thirds of the spanwise computational stations were on the blade; the remainder were in the field inboard and outboard of the blade tip. Using an efficient, fully vectorized version of the code on a CRAY 1S computer, computation times of 20-30 sec per case for the straight blade, and 40-50 sec for the swept-tip configuration were obtained.

## RESULTS AND DISCUSSION

The results of the ROT22 computations were compared with the ONERA measurements at blade azimuth angles of 30°, 60°, 90°, 120°, 150°, 180°, and 270° for advance ratios of 0.40 and 0.45 (see table 1). For the straight blade, the spanwise mesh spacing was adjusted so that a computational plane was located at the middle instrumented station (0.892) while for the swept-tip blade, the crank in the tip (0.857 station) was matched. The pressure coefficients were linearly interpolated between the nearest computational stations for the other two radial stations. The pressure coefficient was defined as

$$C_p = \frac{1}{0.7M_s^2} \left( \frac{p}{p_\infty} - 1 \right) \quad (1)$$

where the section Mach number was

$$M_s = (\omega r_s + V_\infty \sin \psi) / a_\infty \quad (2)$$

Here  $V_\infty$  was the forward flight speed,  $a_\infty$  the free-stream speed of sound,  $\omega$  the blade rotation rate, and the subscript  $s$  refers to the blade radial station.

Theory and experiment compared well for the straight blade at an advance ratio of 0.4 at all azimuth angles except 270°<sup>1</sup> (see figs. 3(a)-3(g)). At the important 90° position (fig. 3(c)), the tip Mach number was 0.84, resulting in a sizable region of supersonic flow. However, at 120° the flow was entirely subsonic. At the higher advance ratio of 0.45, and a maximum tip Mach number of 0.87, agreement with the data was again good (figs. 3(h)-3(n)). The exception was at 120° where a pocket of supersonic flow was present near the leading edge, and the subsequent shock persisted longer than was calculated; this caused the peak expansion pressures to be somewhat underpredicted.

The swept-tip blade represents a more complex geometry than the straight, and experienced higher tip Mach numbers since the tip speed was increased from 200 m/sec to 210 m/sec. At the advance ratio of 0.40, the maximum tip Mach number was 0.88, and at 0.45 it was 0.91. In general, the agreement was not as good as for the straight blade; however, there was also more scatter in the data for the swept-tip cases. Still, agreement at both advance ratios (figs. 4(a)-4(n)) was good in the first quadrant to about 60° and in the second quadrant beyond 120°. At 90° (figs. 4(c) and 4(j)), at the station where the crank in the planform occurs, the pressure expansion rate near the leading edge is somewhat overpredicted; however, it is possible that viscous effects were responsible due to the abrupt change in leading edge sweep. At 120° (figs. 4(d) and 4(k)), the tendency of the supersonic region and its terminating shock to persist longer and be stronger (the shock was farther aft) than predicted by the quasi-steady calculation is noticeable. The combination of the 30° tip sweep angle and the 120° azimuth angle resulted in peak Mach numbers on the blade

---

<sup>1</sup>At 270° there was much scatter in the data for all cases since the pressures were below the sensitivity range of the gauges. While ROT22 does not treat the reverse flow, inboard region, of the blade accurately, the calculation of the flow on the outboard part of the blade should not be strongly affected by the inaccuracies in the reverse flow region.

surface which were almost as high as those at  $90^\circ$  azimuth. Therefore, the region of supersonic flow persisted farther into the second quadrant when the tip was swept back, as was previously discussed in reference 8.

## CONCLUSIONS

Calculations from the ROT22 quasi-steady full potential rotor flow field code were compared with pressure distributions measured by ONERA on straight- and swept-tip model rotors at advance ratios of 0.40 and 0.45.

For the straight blade at an advance ratio of 0.4 (corresponding to a tip Mach number of 0.84 at  $90^\circ$  azimuth), the calculated and measured pressures agreed well. At the higher advance ratio of 0.45 (corresponding to a peak tip Mach number of 0.87), agreement was still good, except at  $120^\circ$  where the supersonic region and the shock persisted longer than predicted by the quasi-steady calculation. The importance of the unsteady effects for this case was also shown in reference 10 using time-dependent small disturbance theory.

For the swept-tip blade at the 0.4 advance ratio, the tip Mach number was 0.88 at  $90^\circ$  azimuth and for the 0.45 advance ratio it was 0.91. For both advance ratios, agreement was good to azimuth angles of about  $60^\circ$  and beyond  $120^\circ$ . At  $90^\circ$ , the pressures were somewhat overpredicted, especially near the crank in the tip. At  $120^\circ$ , the shock strength and locations were underpredicted by the quasi-steady code.

In summary, the unsteadiness of the flow affected shock waves and their position most in the second quadrant, beyond  $90^\circ$  azimuth. When the combination of tip Mach number, advance ratio, and airfoil thickness ratio produced relatively weak shocks, the ROT22 code gave good results. However, when the shocks were strong, they persisted longer on the blade than predicted by the quasi-steady calculation; this was especially noticeable at the  $120^\circ$  blade position.



## REFERENCES

1. Caradonna, F. X.; and Isom, M. P.: Subsonic and Transonic Potential Flow over Helicopter Rotor Blades. AIAA Journal, vol. 10, no. 12, Dec. 1972, pp. 1606-1612.
2. Caradonna, F. X.; and Isom, M. P.: Numerical Calculation of Unsteady Transonic Potential Flow over Helicopter Rotor Blades. AIAA Journal, vol. 14, no. 4, Apr. 1976.
3. Grant, J.: Calculation of the Supercritical Flow over the Tip Region of a Non-Lifting Rotor Blade at Arbitrary Azimuth. Royal Aircraft Establishment Technical Report 77180, Dec. 1977.
4. Jameson, A.; and Caughey, D. A.: Numerical Calculation of the Transonic Flow Past a Swept Wing. Courant Institute of Mathematical Sciences, COO-3077-140, New York University, N.Y., June 1977.
5. Arieli, R.; and Tauber, M. E.: Computation of Subsonic and Transonic Flow about Lifting Rotor Blades. AIAA Paper 79-1667, Aug. 1979.
6. Arieli, R.; and Tauber, M. E.: Analysis of the Quasi-Steady Flow about an Isolated Lifting Helicopter Rotor Blade. Joint Institute for Aeronautics and Acoustics TR-24, Stanford University, Aug. 1979.
7. Caradonna, F. X.; and Philippe, J. J.: The Flow over a Helicopter Blade Tip in the Transonic Regime. Vertica, vol. 2, 1978, pp. 43-60.
8. Monnerie, B.; and Philippe, J. J.: Aerodynamic Problems of Helicopter Blade Tips. Vertica, vol. 2, 1979, pp. 217-231.
9. Chang, I. C.; and Tauber, M. E.: Numerical Calculation of the Transonic Potential Flow Past a Cranked Wing. NASA TM-84391, 1983.
10. Chattot, J. J.; and Philippe, J. J.: Pressure Distribution Computation on a Nonlifting Symmetrical Helicopter Blade in Forward Flight. La Recherche Aeronautique (English version), no. 1980-5, pp. 19-33.

TABLE 1.- TABLE OF FIGURES

$\psi$	Tip configuration			
	Straight		Swept	
	$\mu$	0.4 0.45	0.4 0.45	
30°	3a	3h	4a	4h
60°	3b	3i	4b	4i
90°	3c	3j	4c	4j
120°	3d	3k	4d	4k
150°	3e	3l	4e	4l
180°	3f	3m	4f	4m
270°	3g	3n	4g	4n

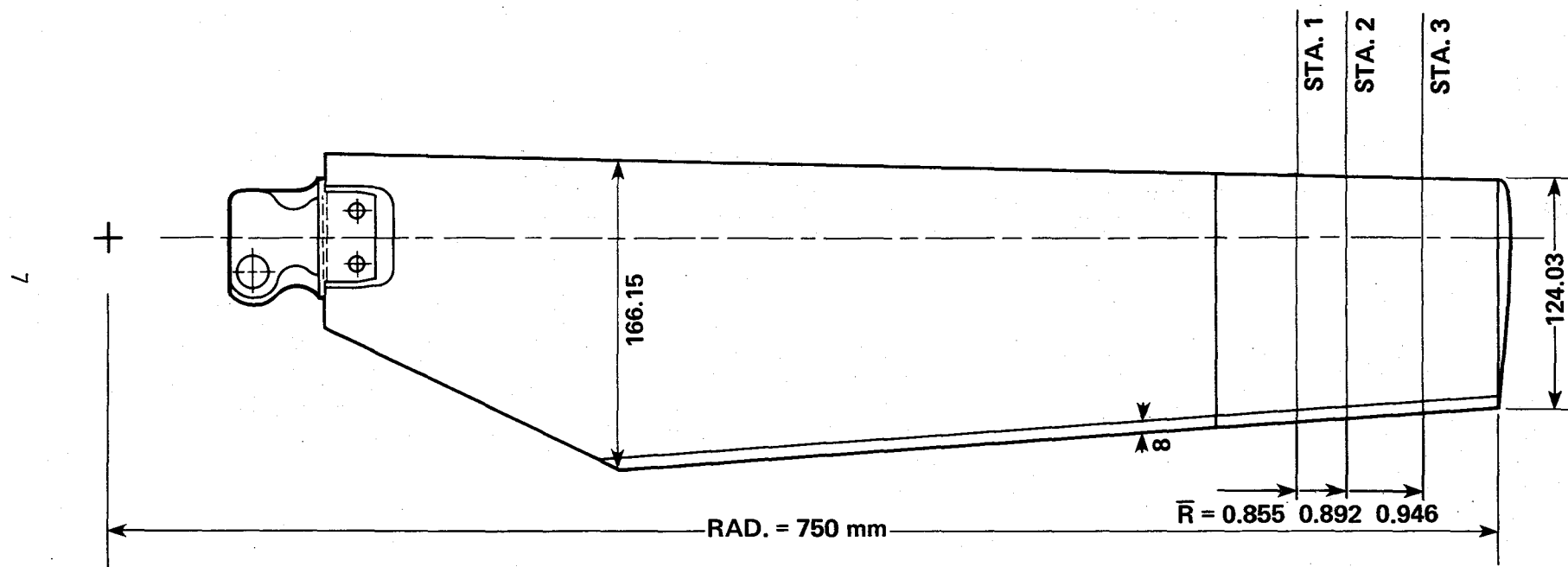


Figure 1.- ONERA straight blade geometry.

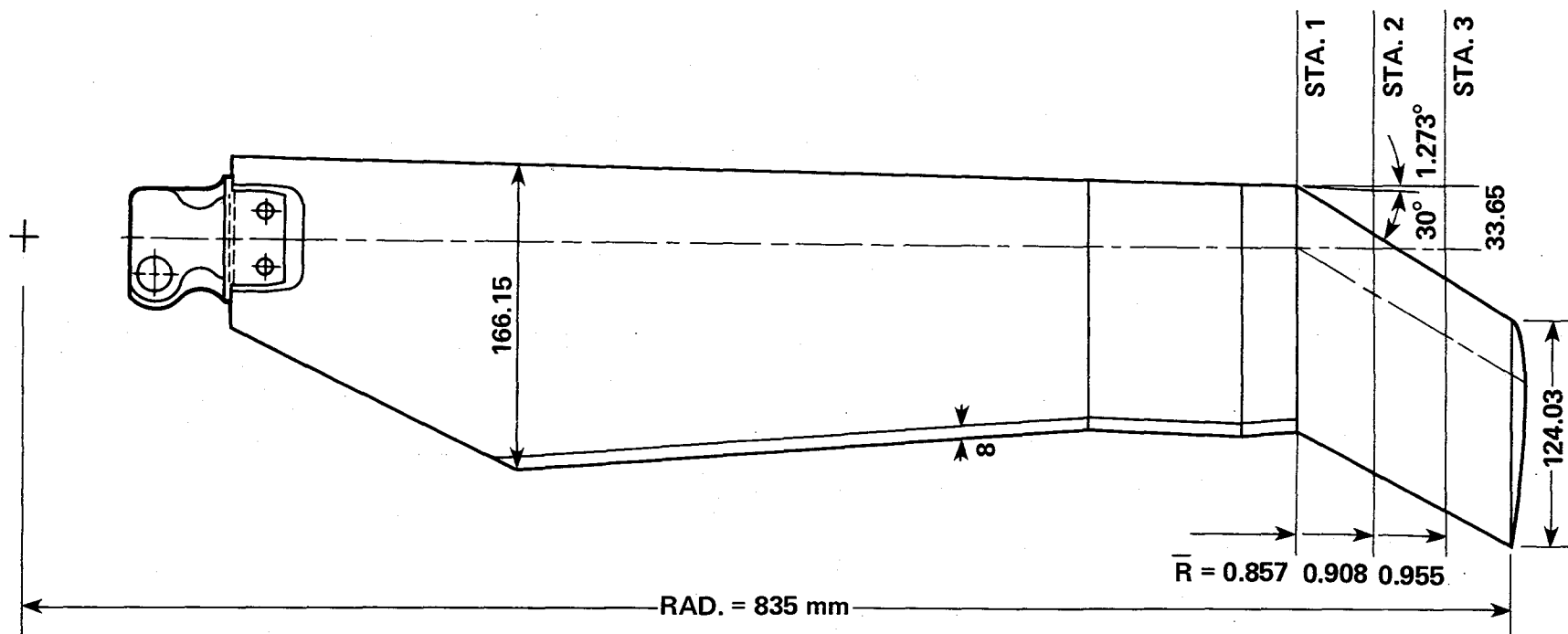
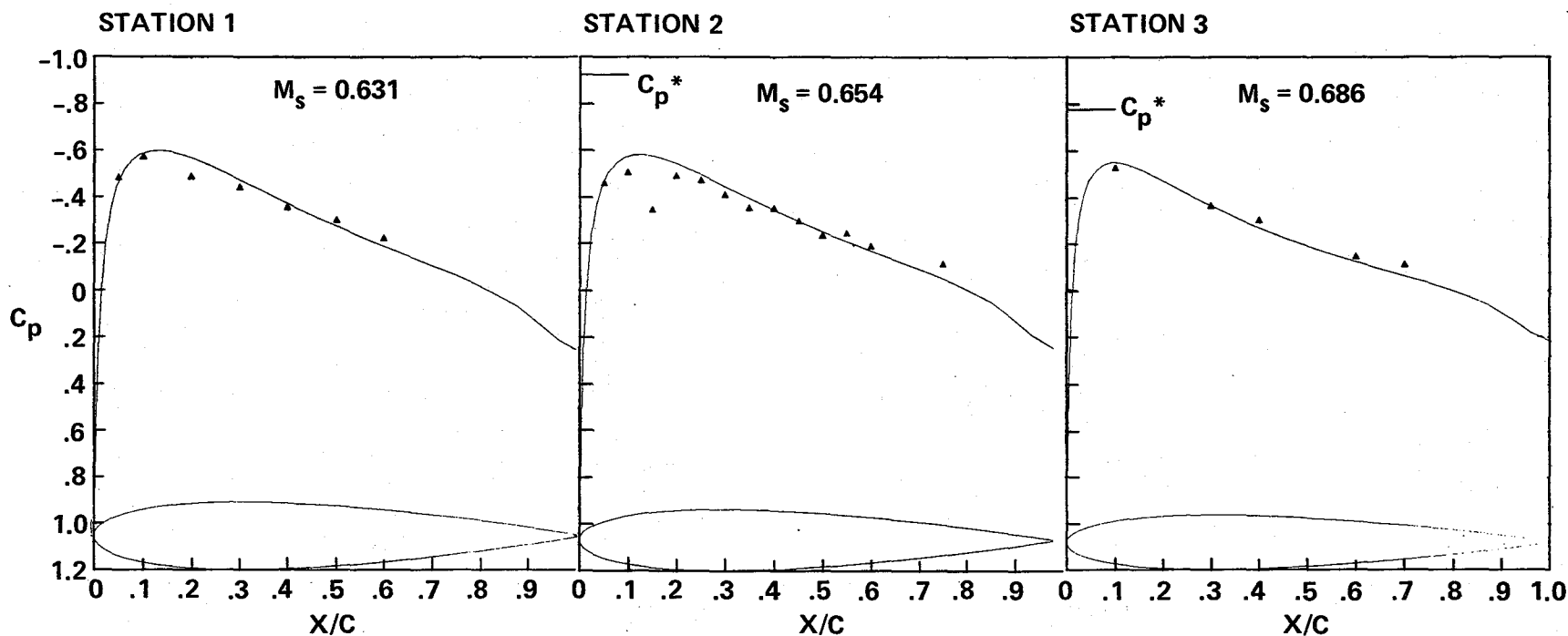
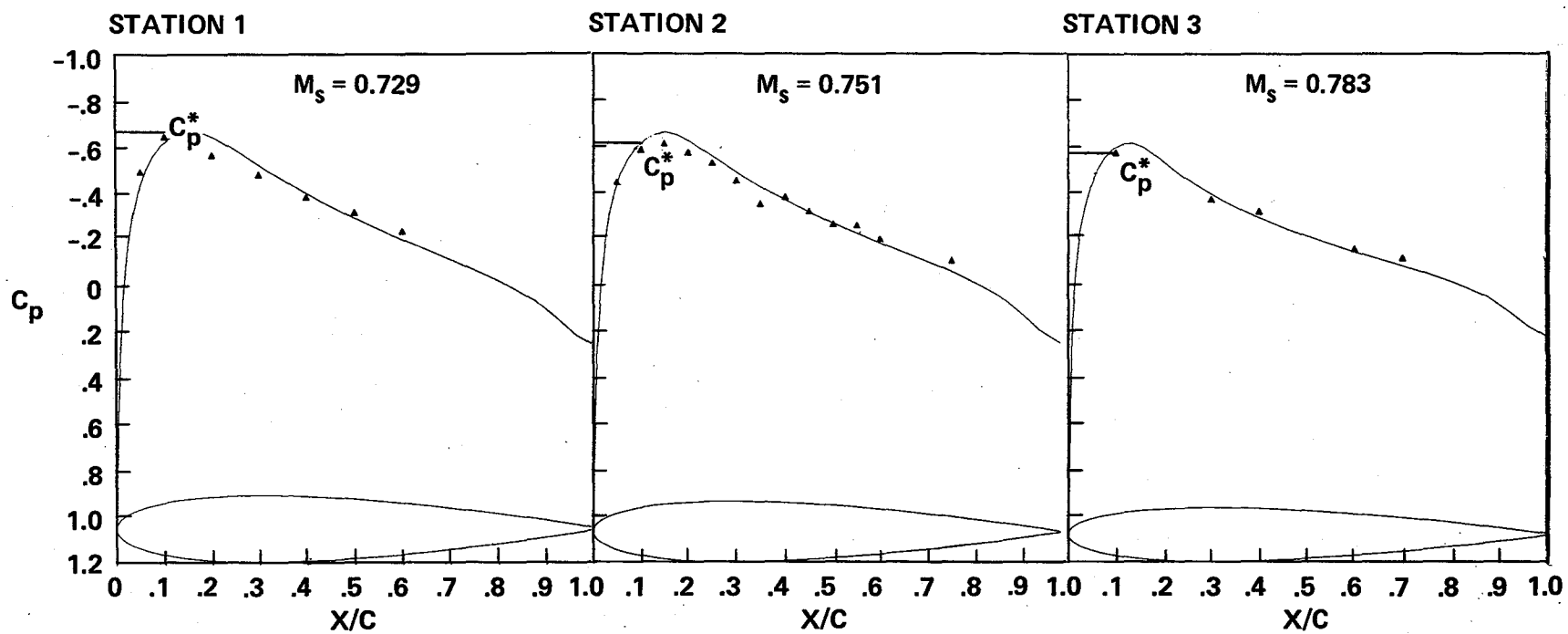


Figure 2.- ONERA swept-tip blade geometry.



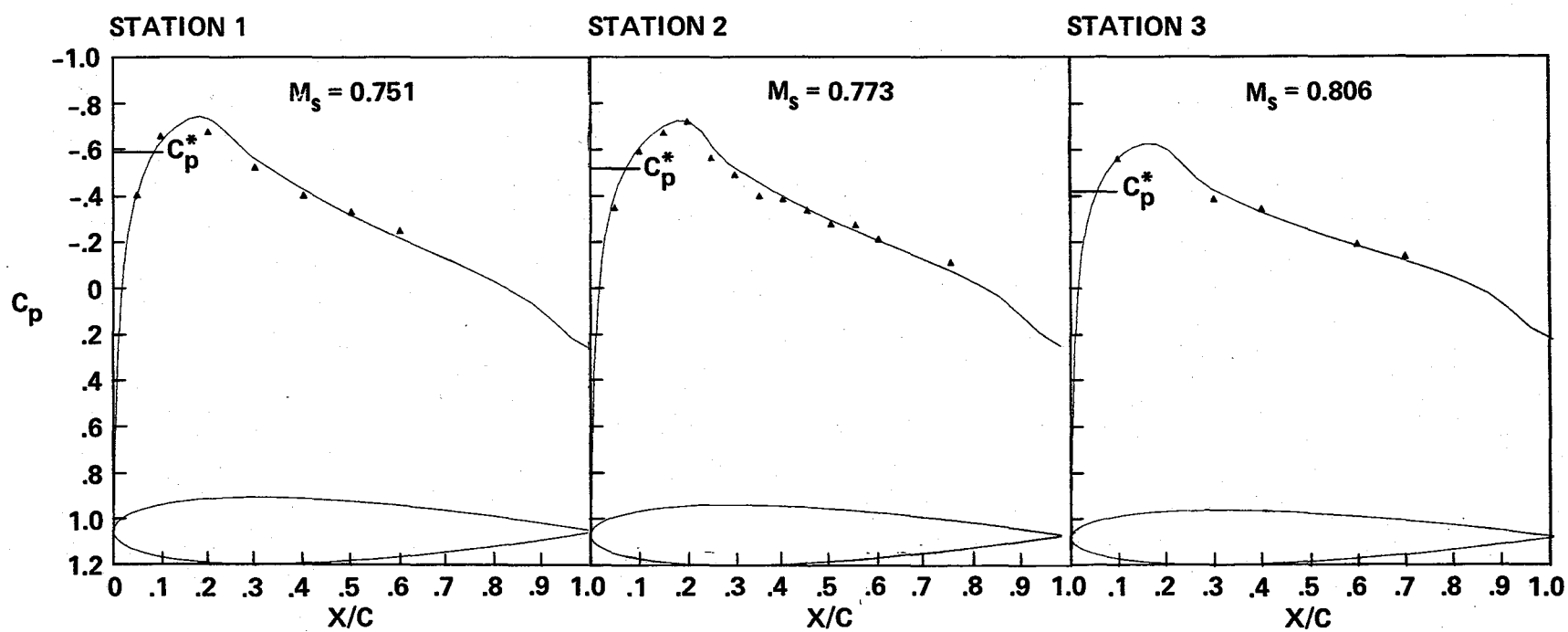
(a)  $\mu = 0.4$ ,  $\psi = 30^\circ$ .

Figure 3.- Theoretical and experimental pressure comparison for straight blades.



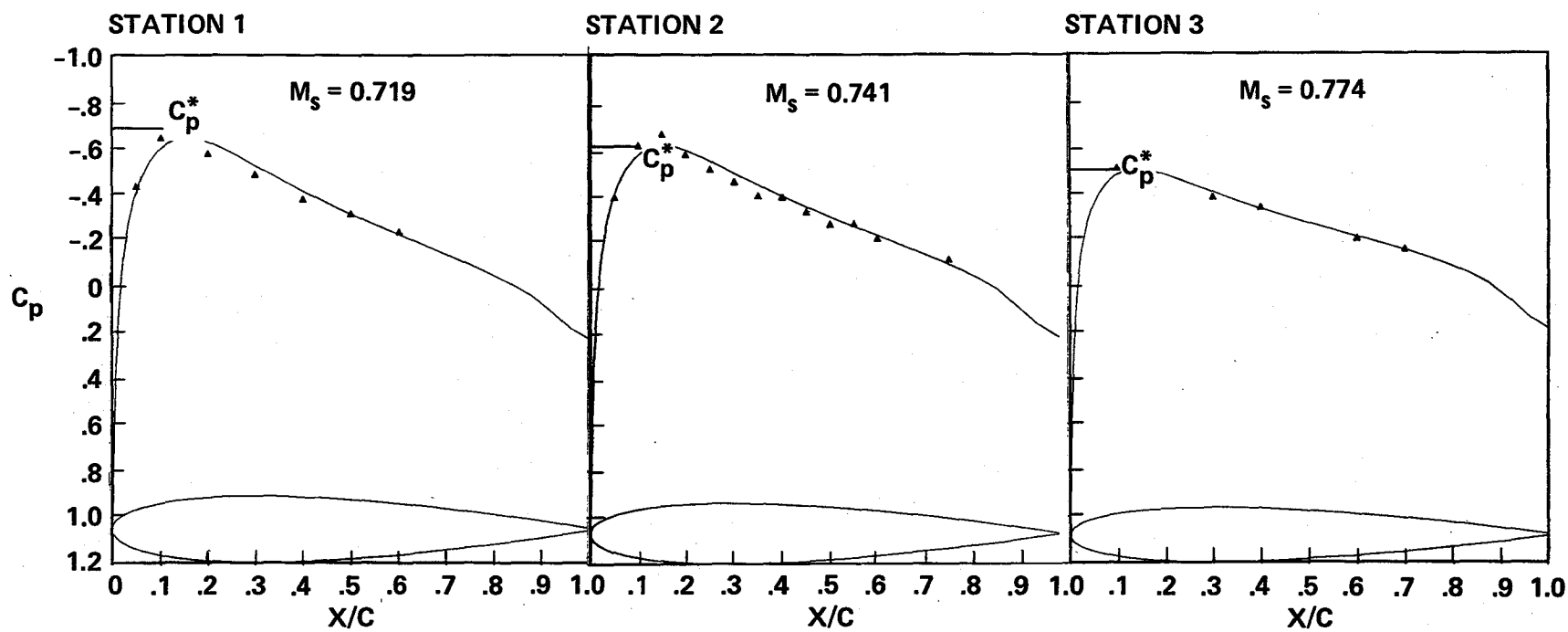
(b)  $\mu = 0.4$ ,  $\psi = 60^\circ$ .

Figure 3.- Continued.



(c)  $\mu = 0.4$ ,  $\psi = 90^\circ$ .

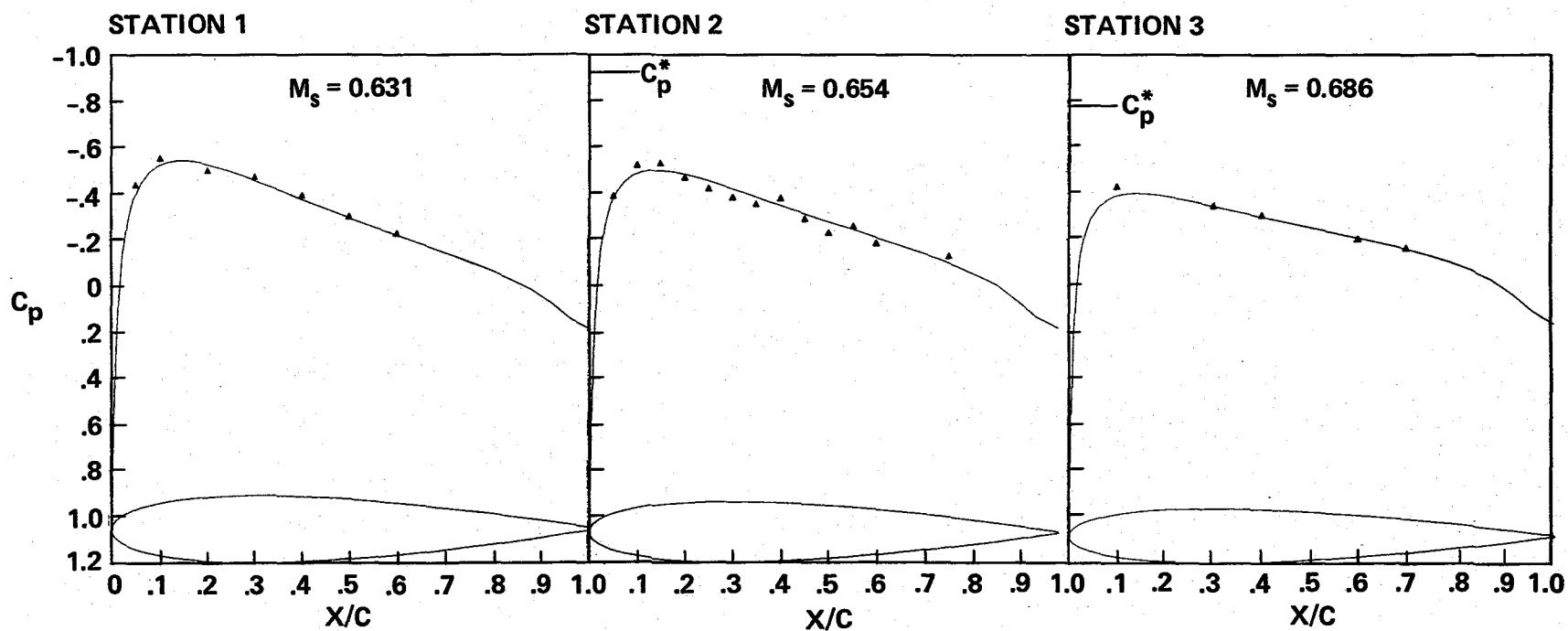
Figure 3.- Continued.



(d)  $\mu = 0.4$ ,  $\psi = 120^\circ$ .

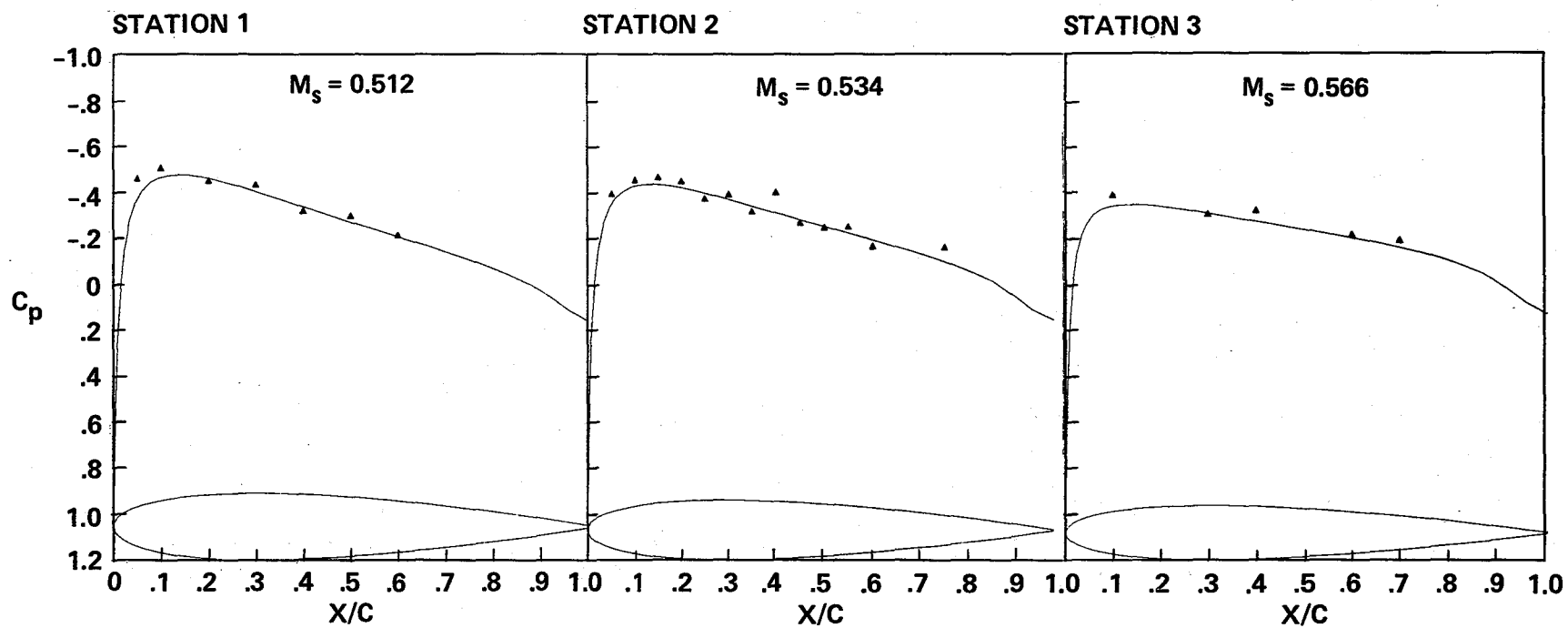
Figure 3.- Continued.





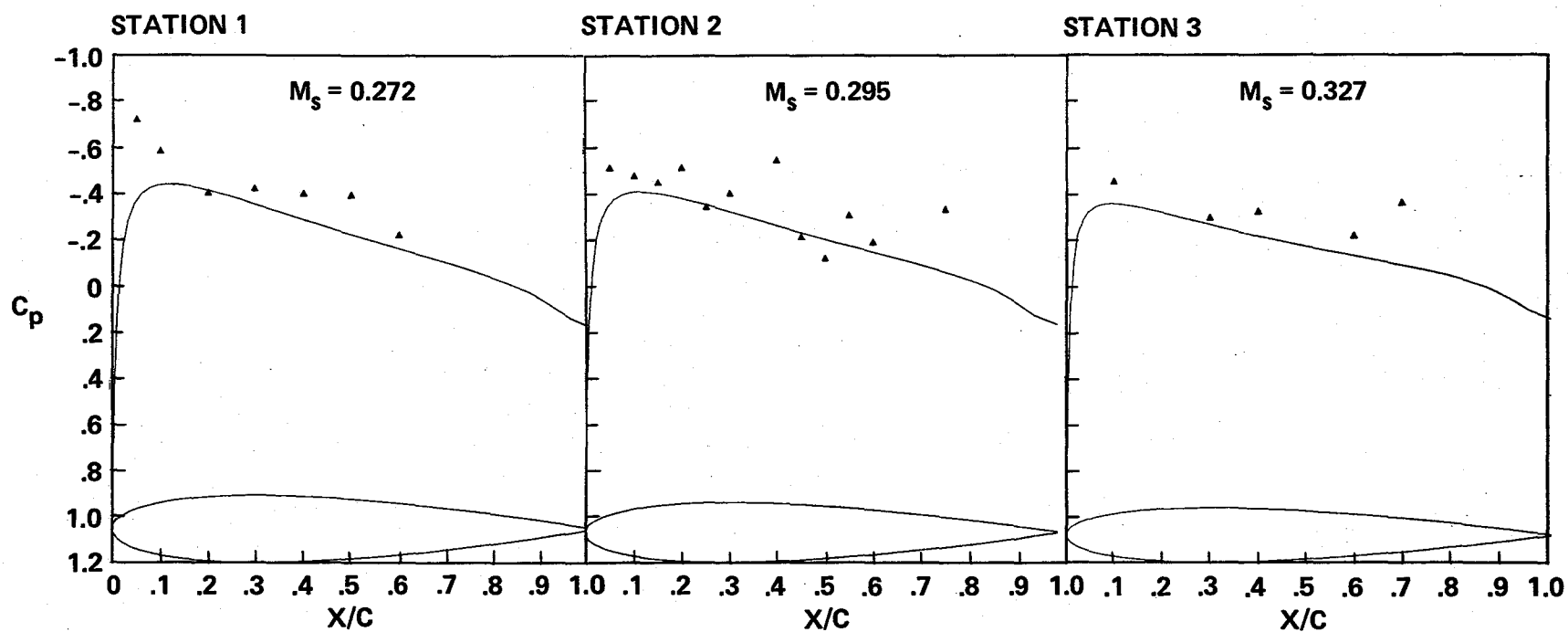
(e)  $\mu = 0.4$ ,  $\psi = 150^\circ$ .

Figure 3.- Continued.



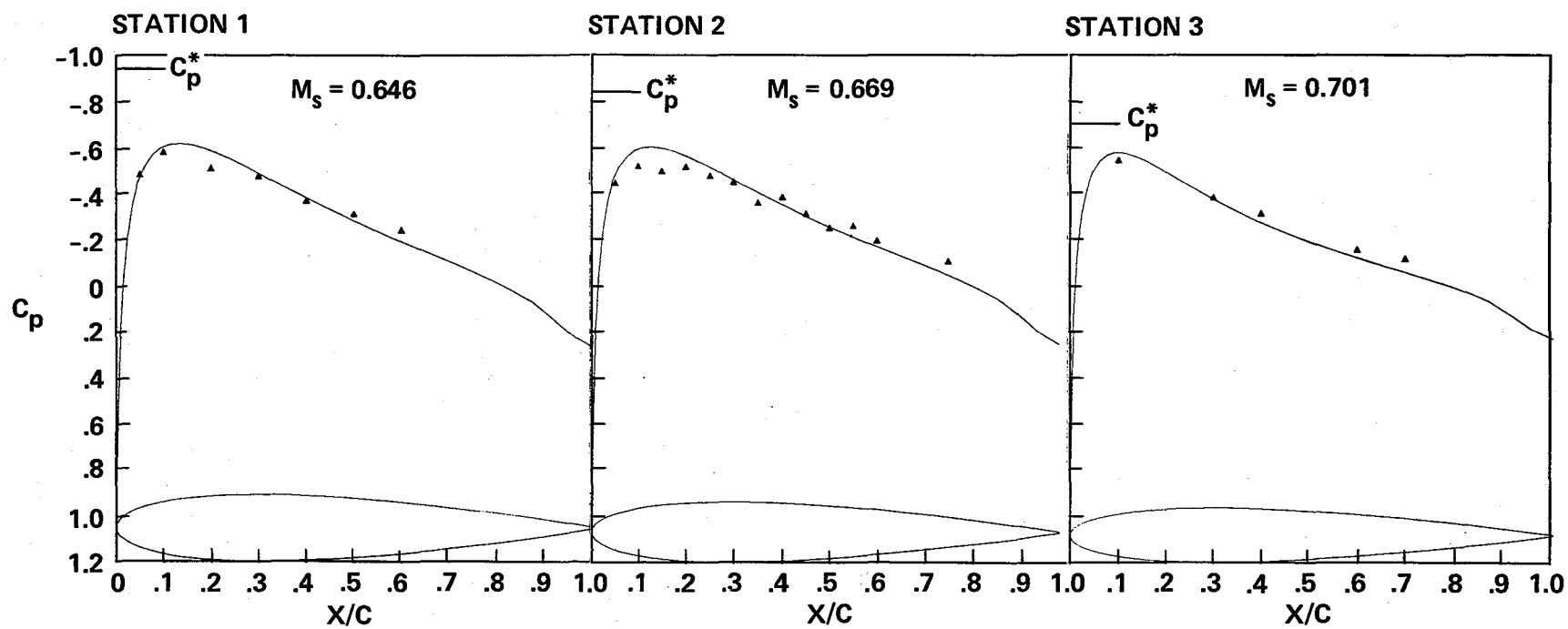
(f)  $\mu = 0.4$ ,  $\psi = 180^\circ$ .

Figure 3.- Continued.



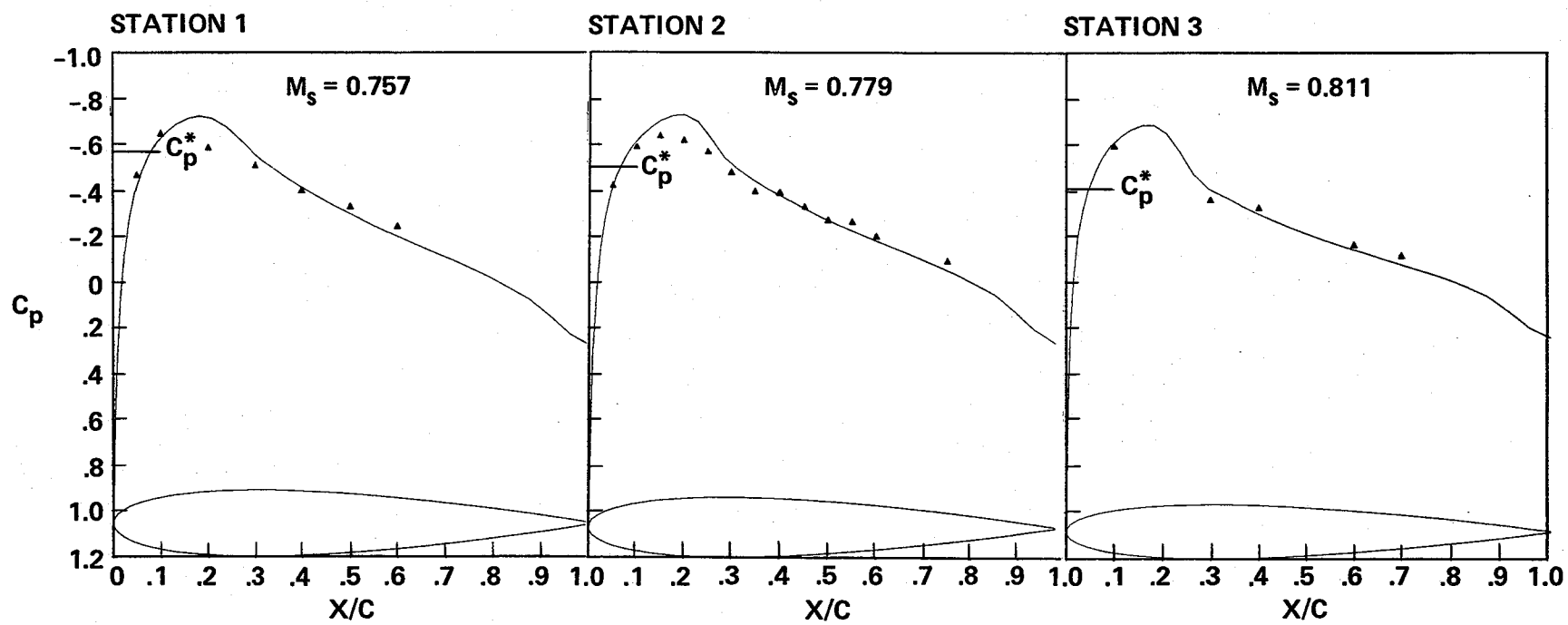
(g)  $\mu = 0.4$ ,  $\psi = 270^\circ$ .

Figure 3.- Continued.



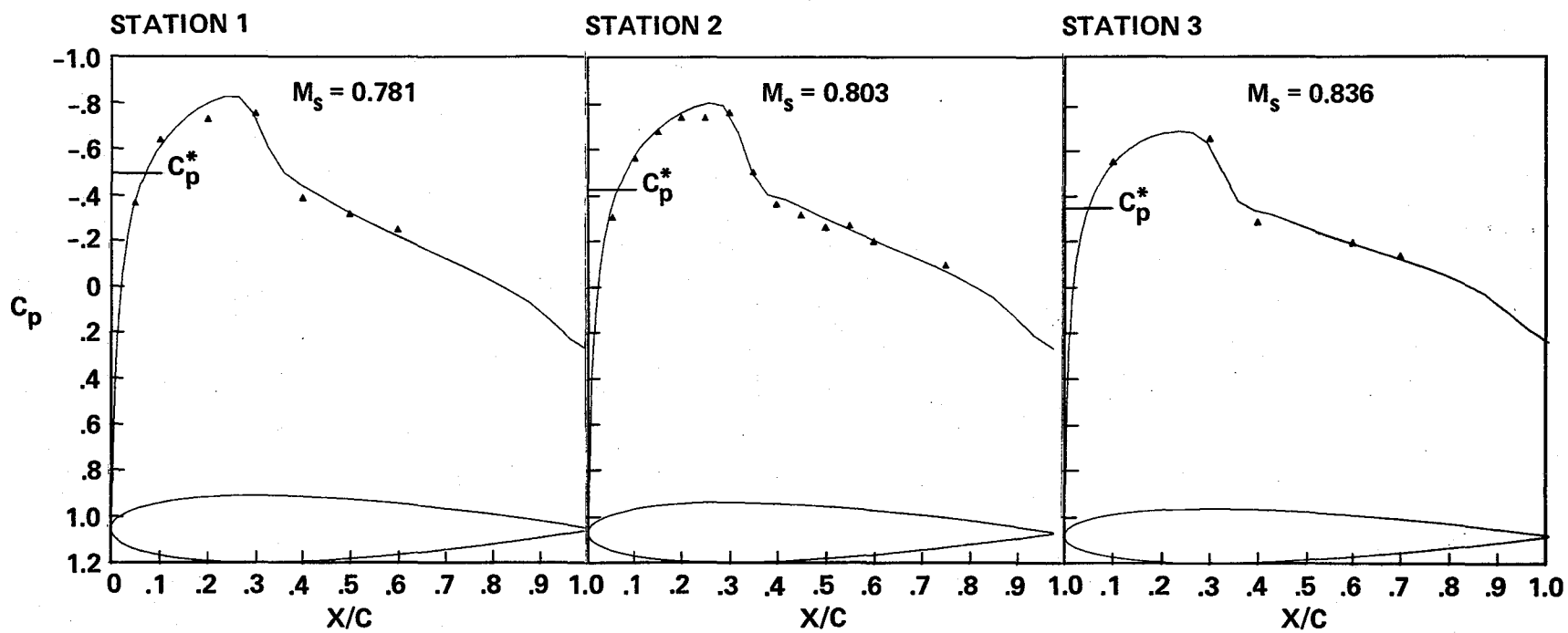
(h)  $\mu = 0.45$ ,  $\psi = 30^\circ$ .

Figure 3.- Continued.



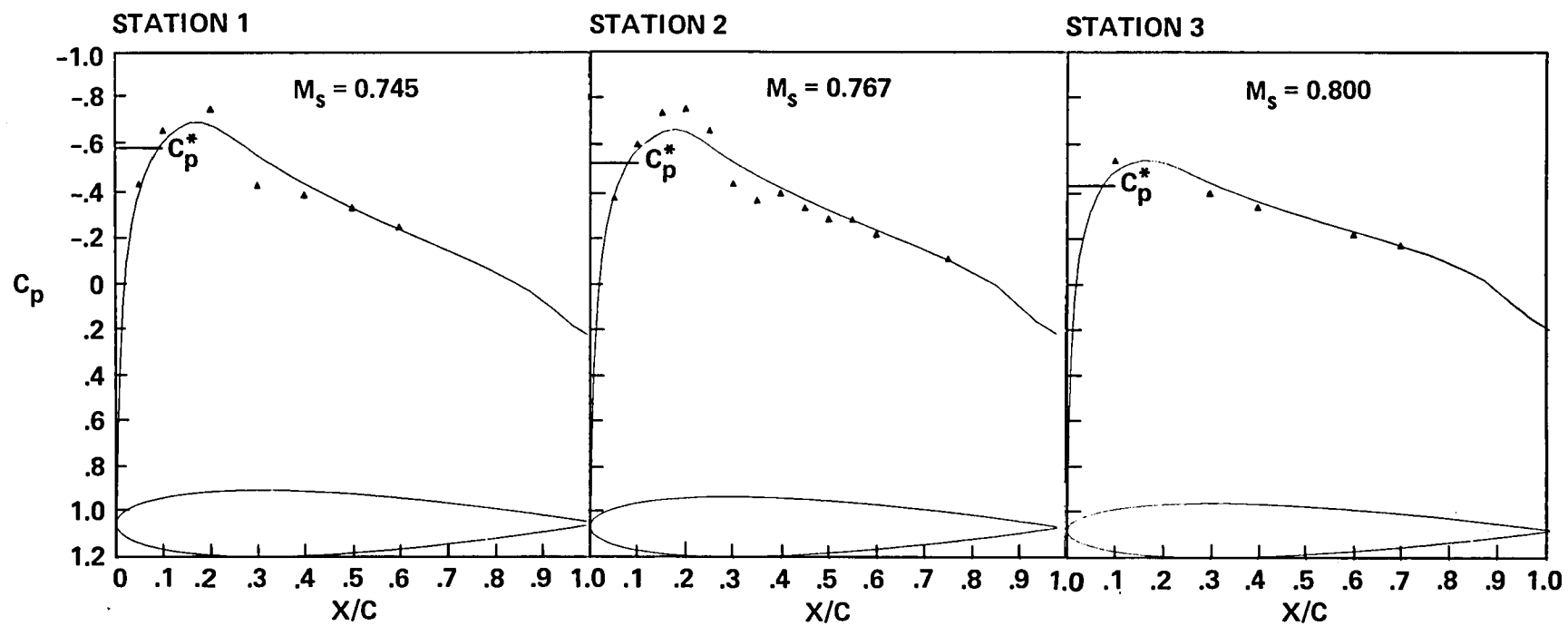
(i)  $\mu = 0.45$ ,  $\psi = 60^\circ$ .

Figure 3.- Continued.



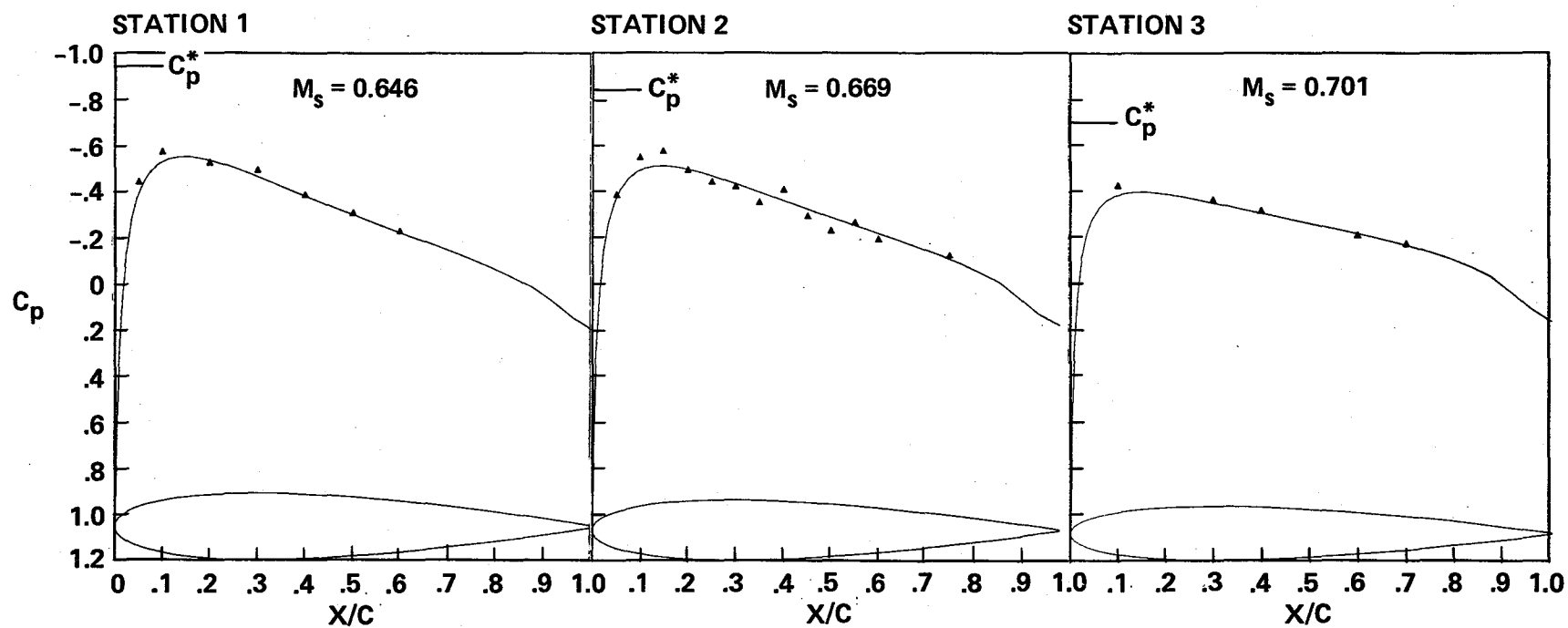
(j)  $\mu = 0.45$ ,  $\psi = 90^\circ$ .

Figure 3.- Continued.



(k)  $\mu = 0.45$ ,  $\psi = 120^\circ$ .

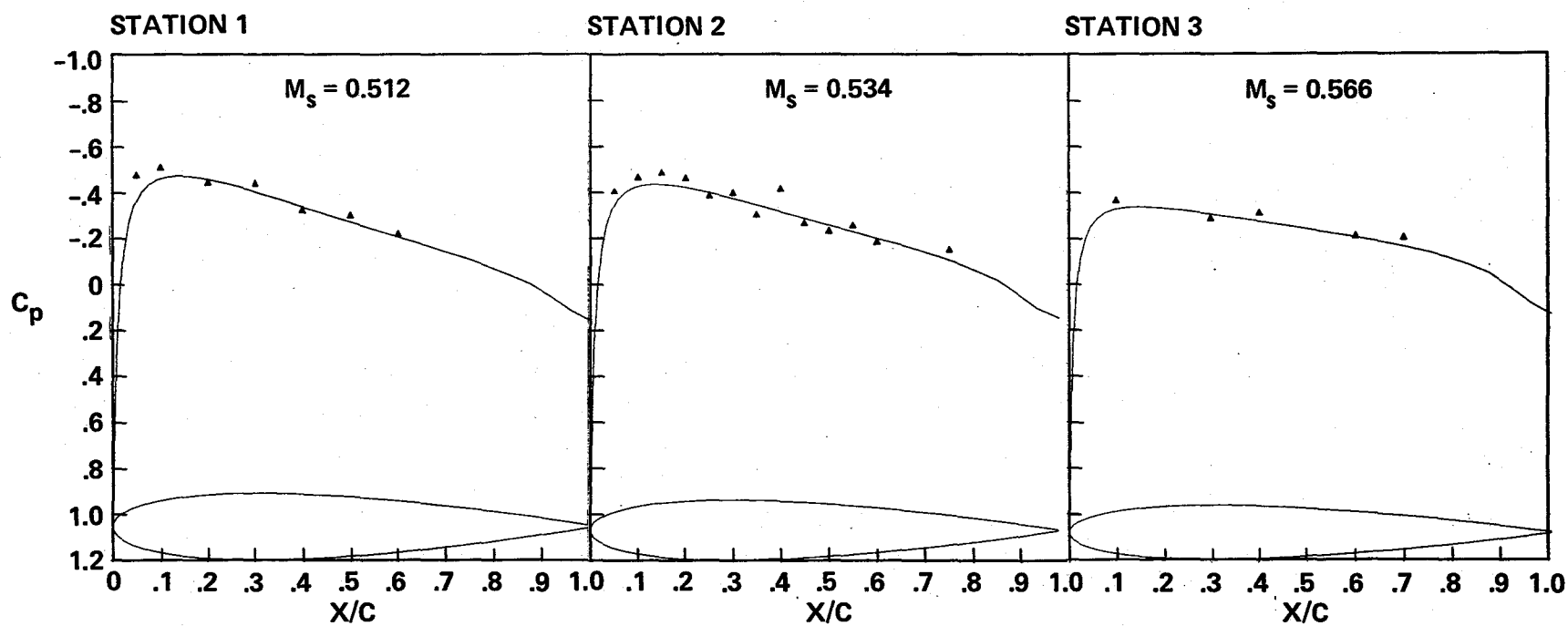
Figure 3.- Continued.



(1)  $\mu = 0.45$ ,  $\psi = 150^\circ$ .

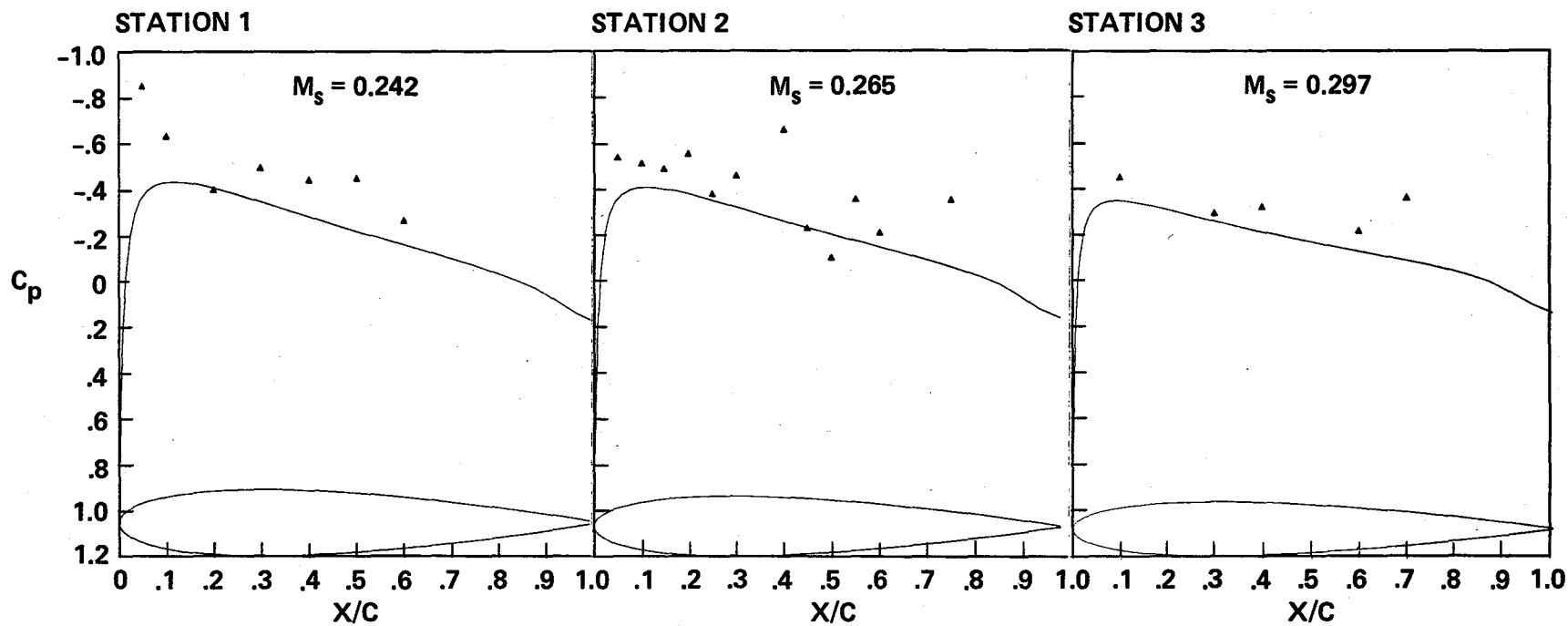
Figure 3.- Continued.





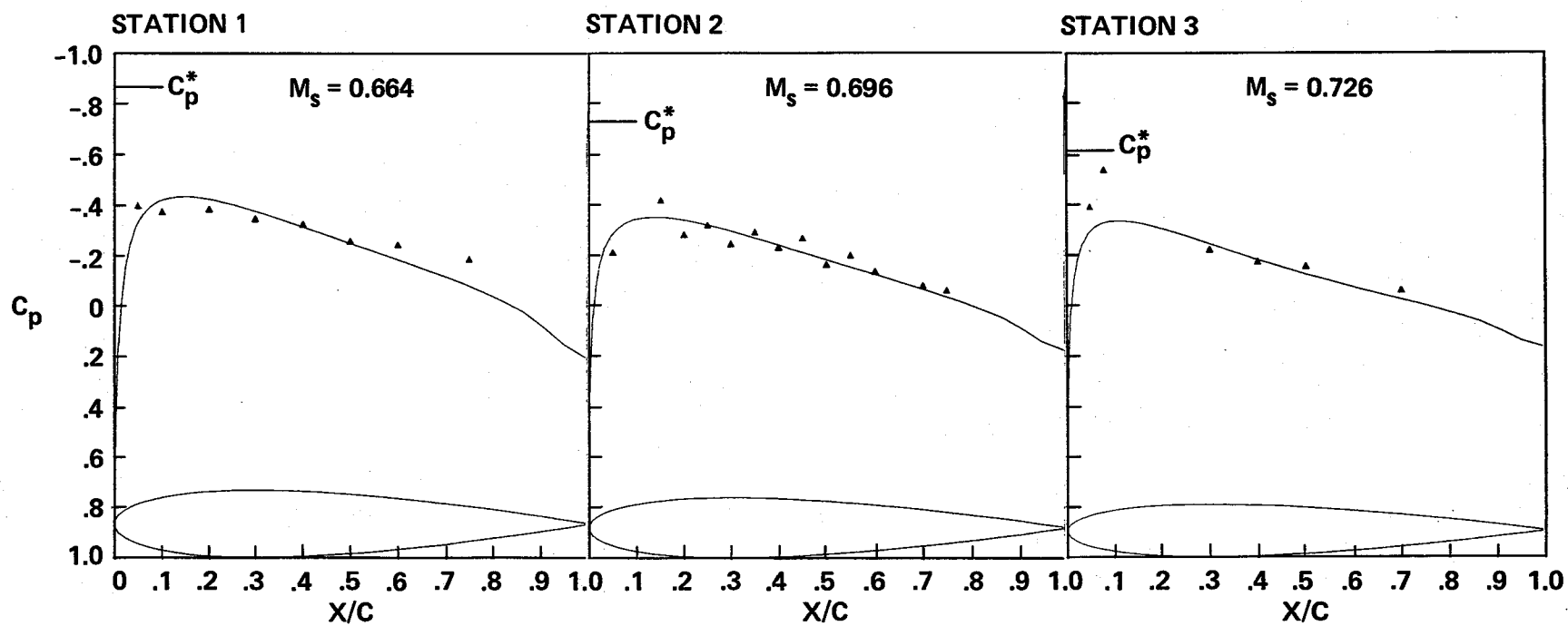
(m)  $\mu = 0.45$ ,  $\psi = 180^\circ$ .

Figure 3.- Continued.



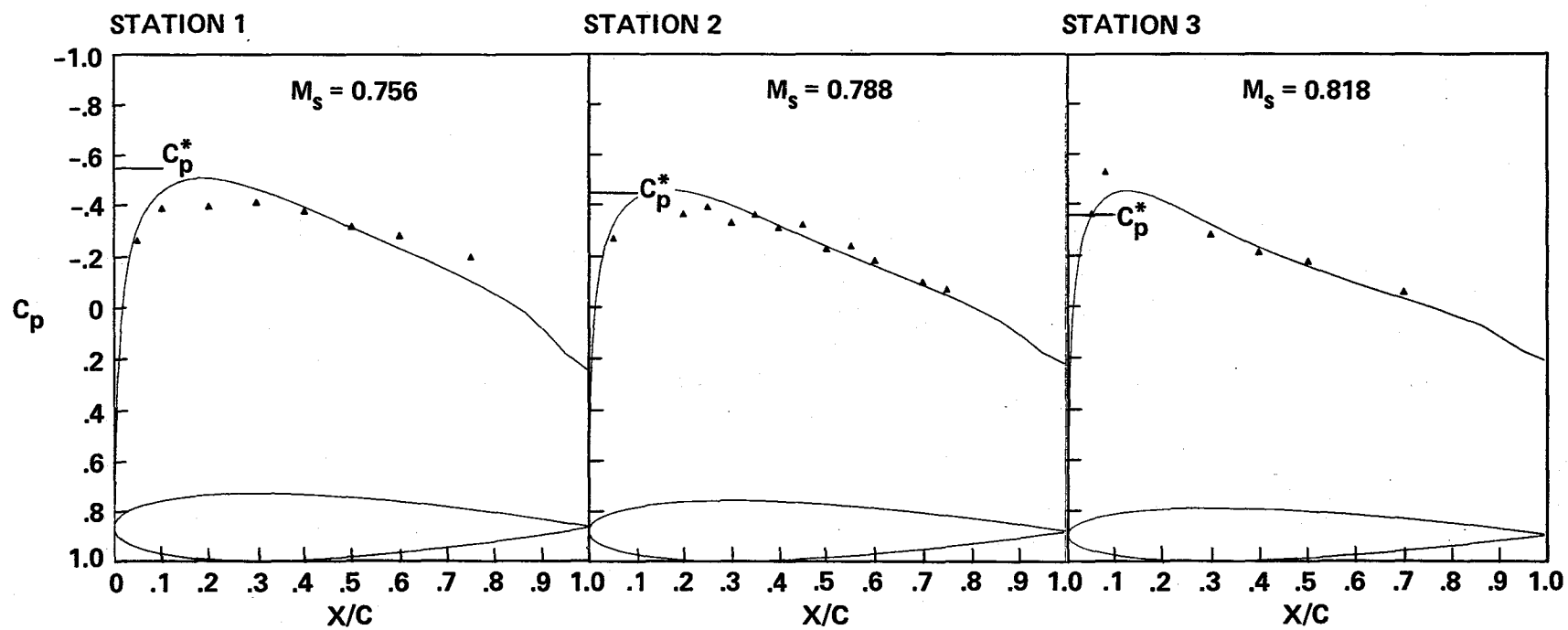
(n)  $\mu = 0.45$ ,  $\psi = 270^\circ$ .

Figure 3.- Concluded.



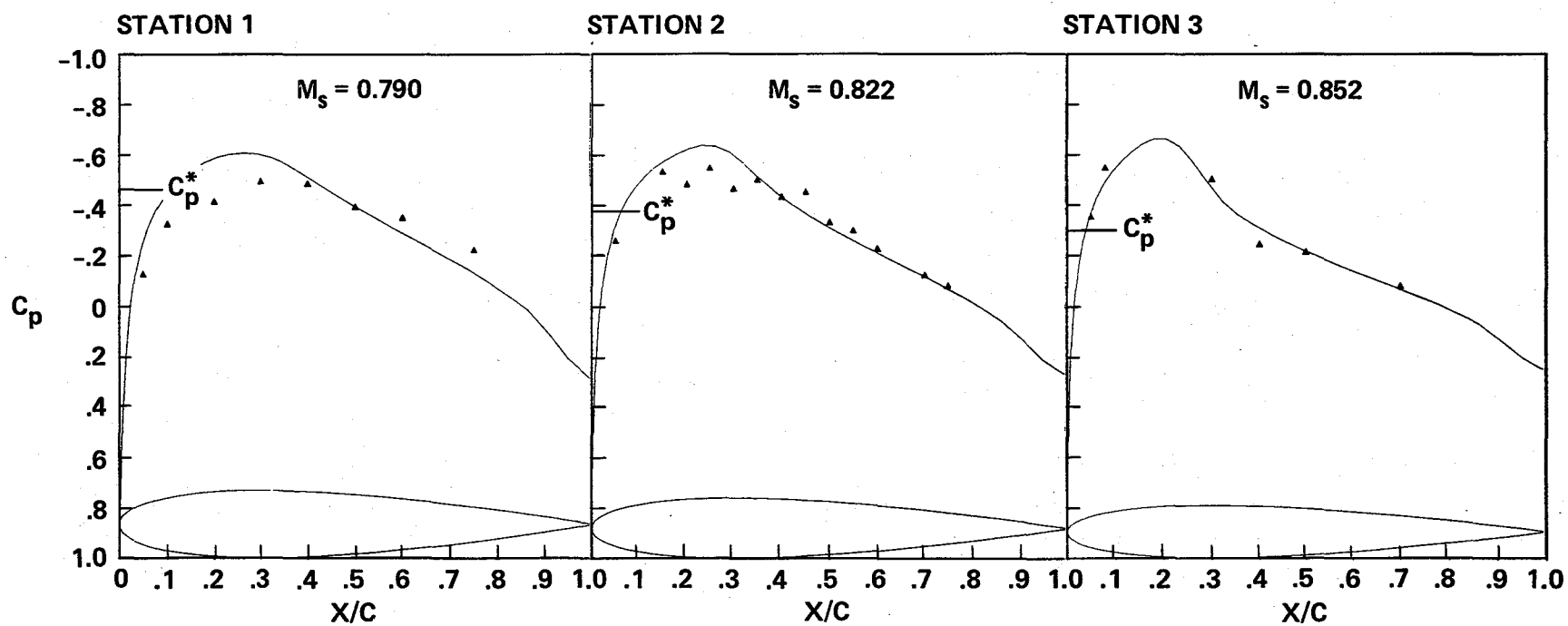
(a)  $\mu = 0.4$ ,  $\psi = 30^\circ$ .

Figure 4.- Theoretical and experimental pressure comparison for swept-tip blades.



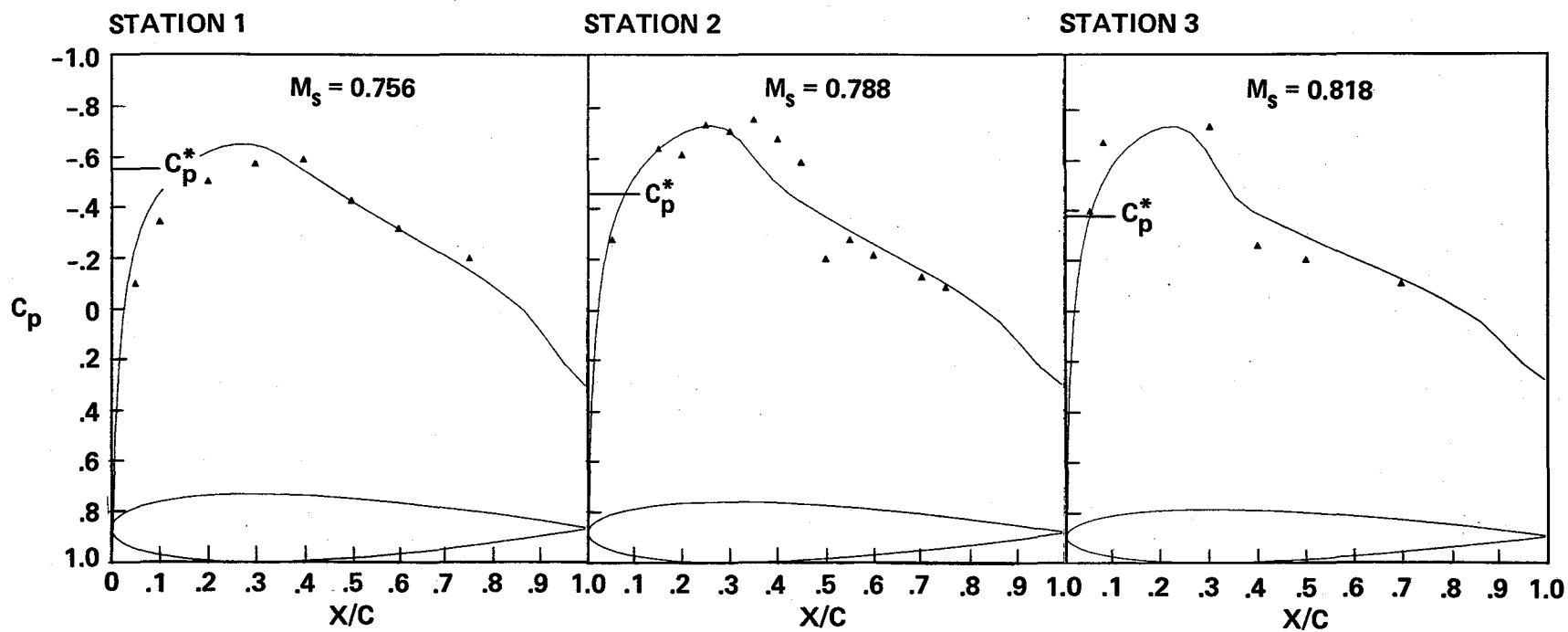
(b)  $\mu = 0.4$ ,  $\psi = 60^\circ$ .

Figure 4.- Continued.



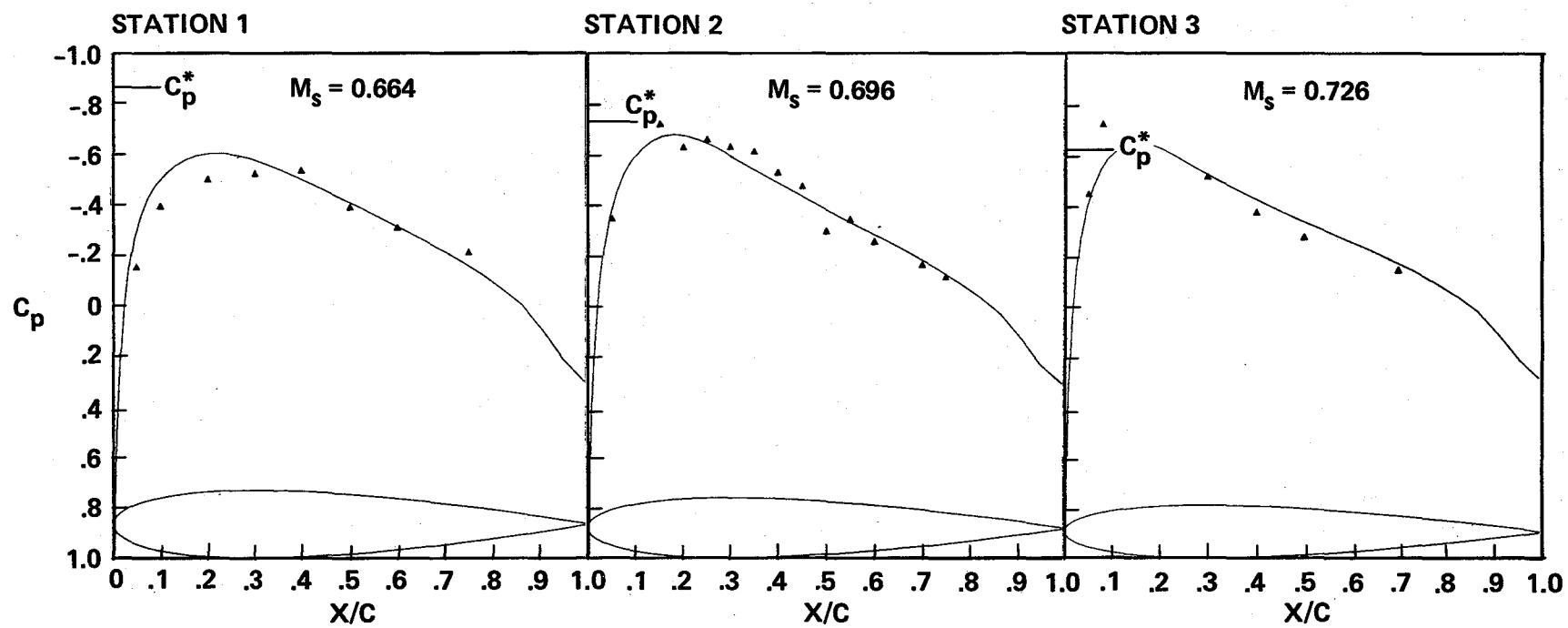
(c)  $\mu = 0.4$ ,  $\psi = 90^\circ$ .

Figure 4.- Continued.



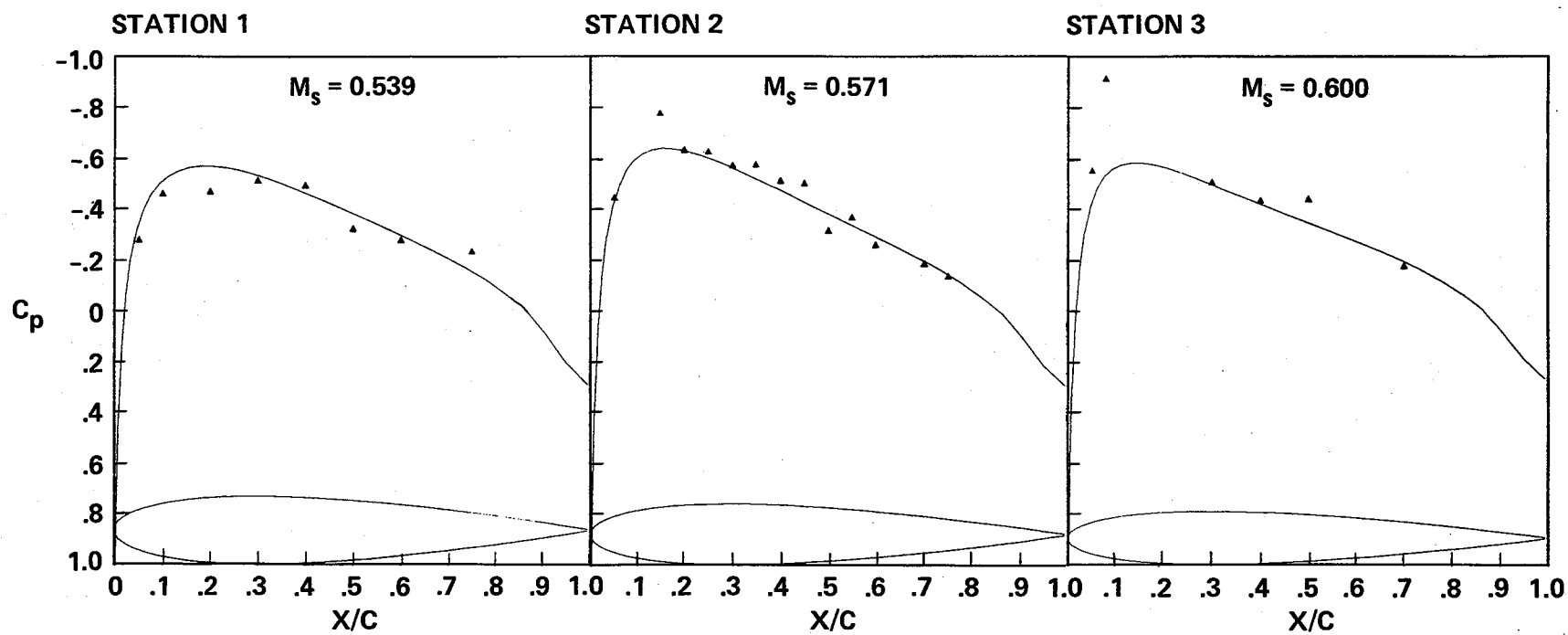
(d)  $\mu = 0.4$ ,  $\psi = 120^\circ$ .

Figure 4.- Continued.



(e)  $\mu = 0.4$ ,  $\psi = 150^\circ$ .

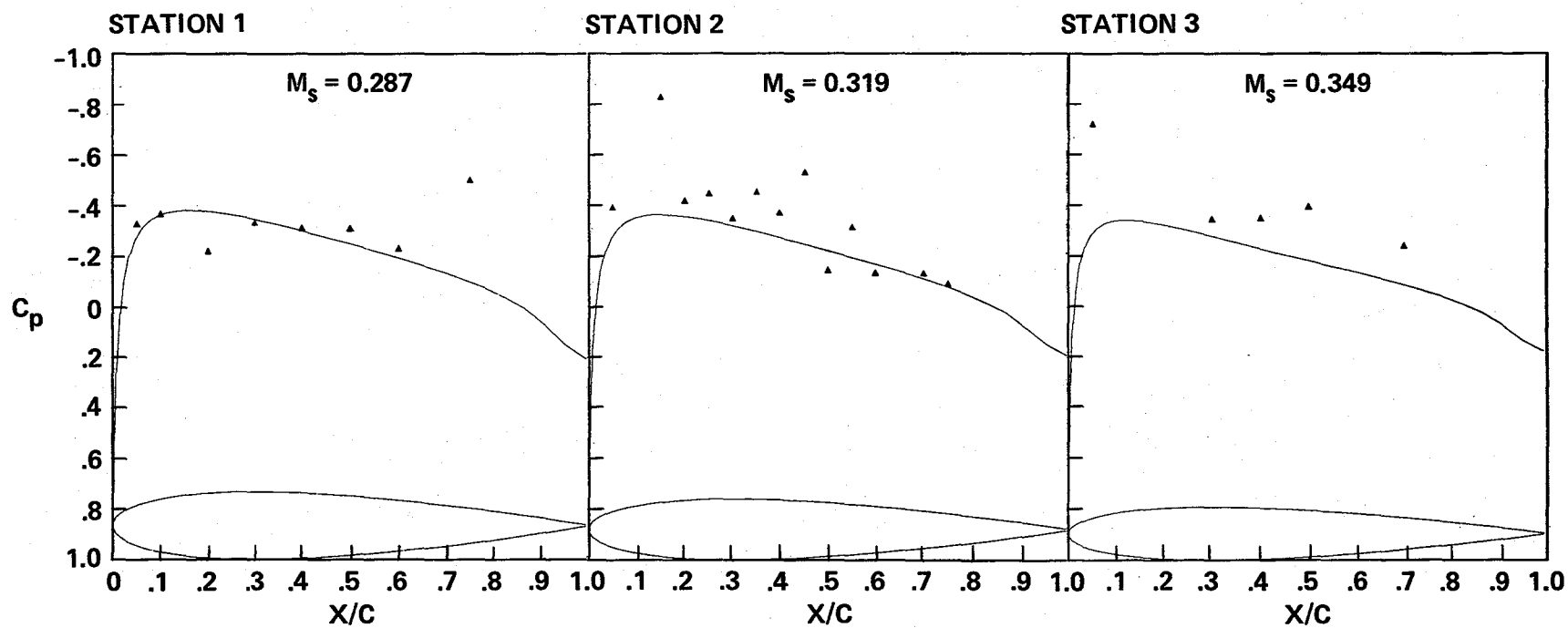
Figure 4.- Continued.



(f)  $\mu = 0.4$ ,  $\psi = 180^\circ$ .

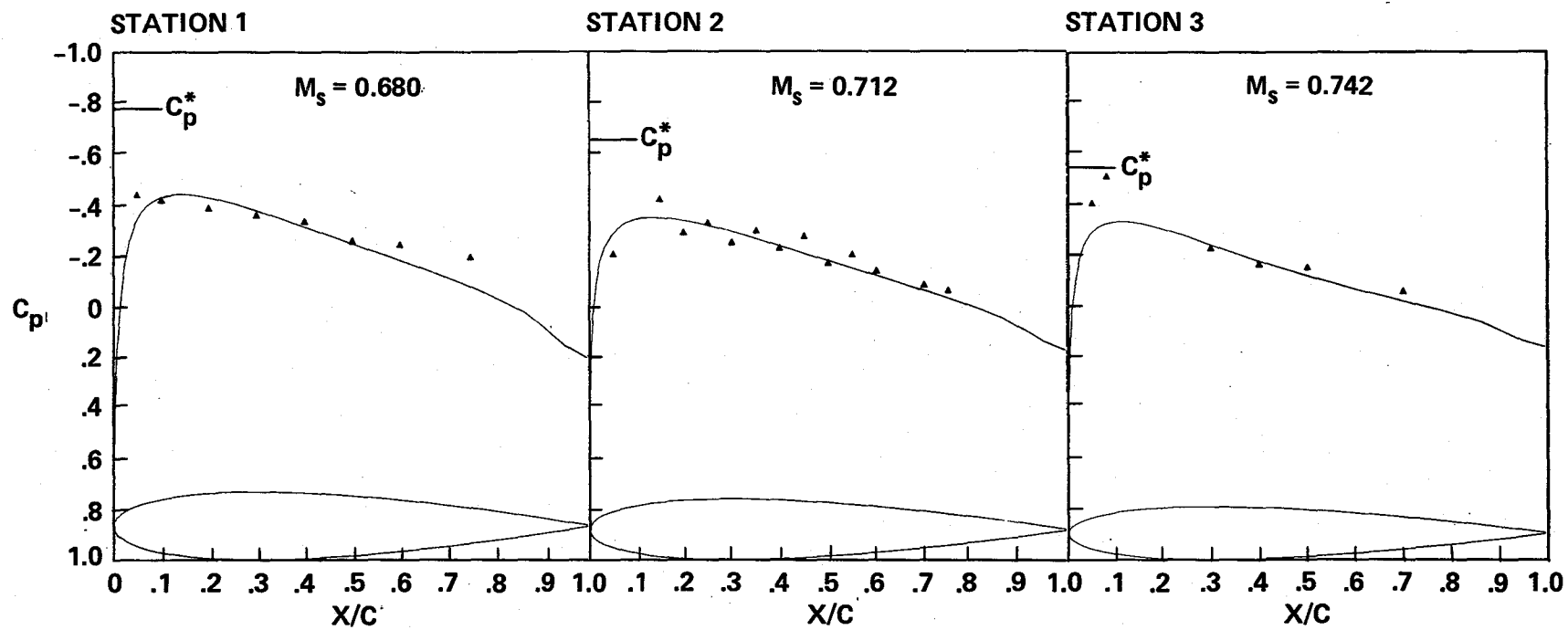
Figure 4.- Continued.





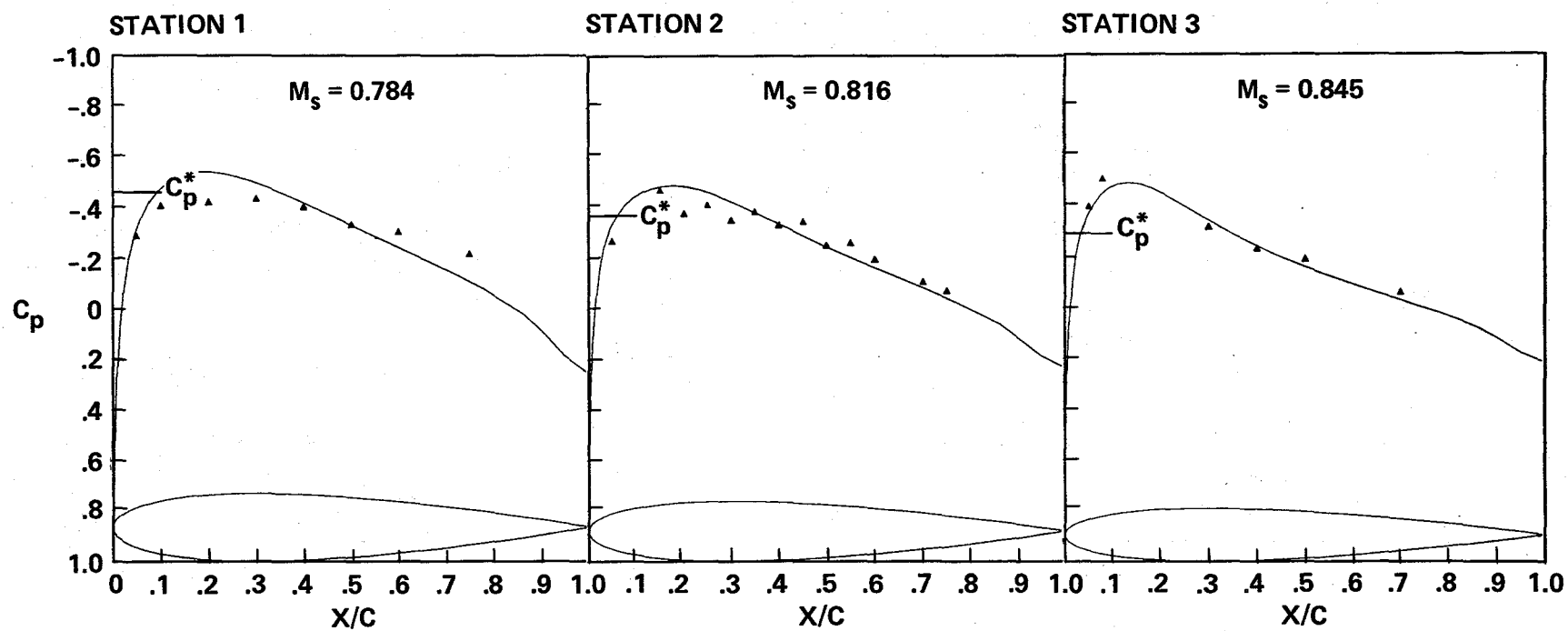
(g)  $\mu = 0.4$ ,  $\psi = 270^\circ$ .

Figure 4.- Continued.



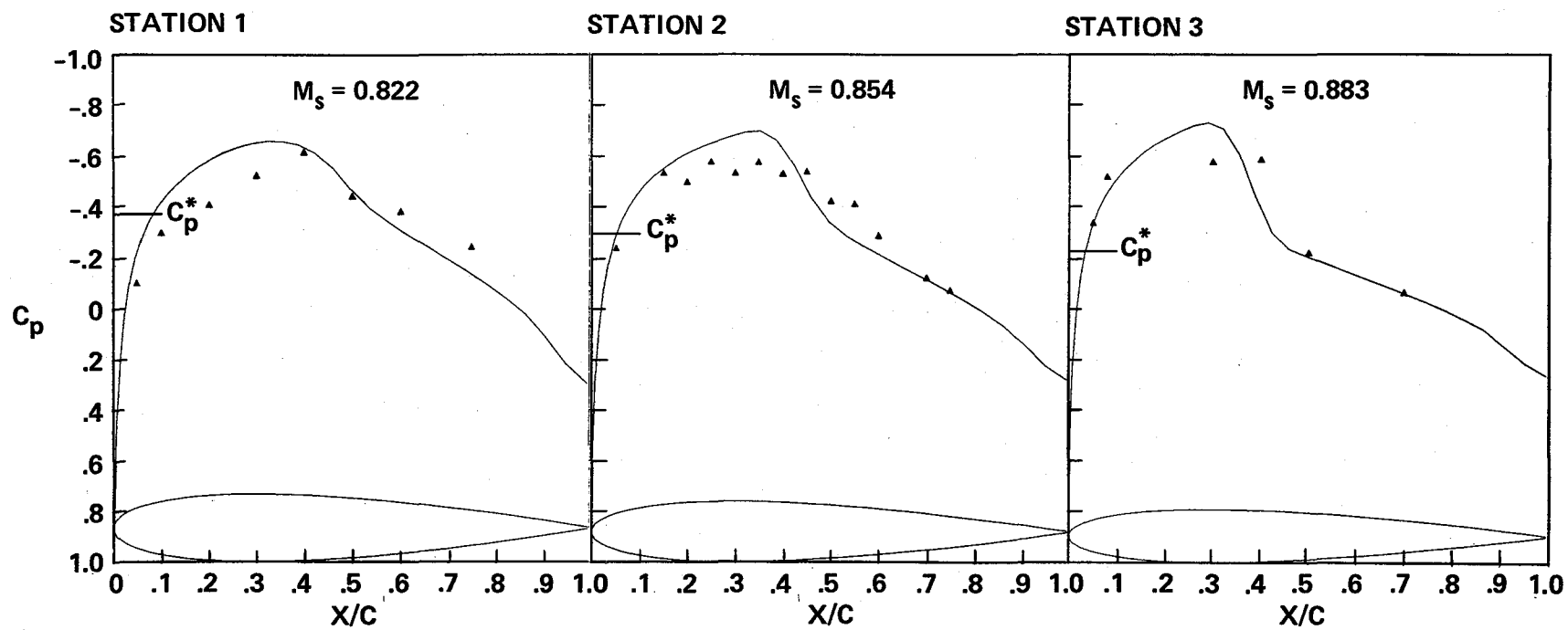
(h)  $\mu = 0.45$ ,  $\psi = 30^\circ$ .

Figure 4.- Continued.



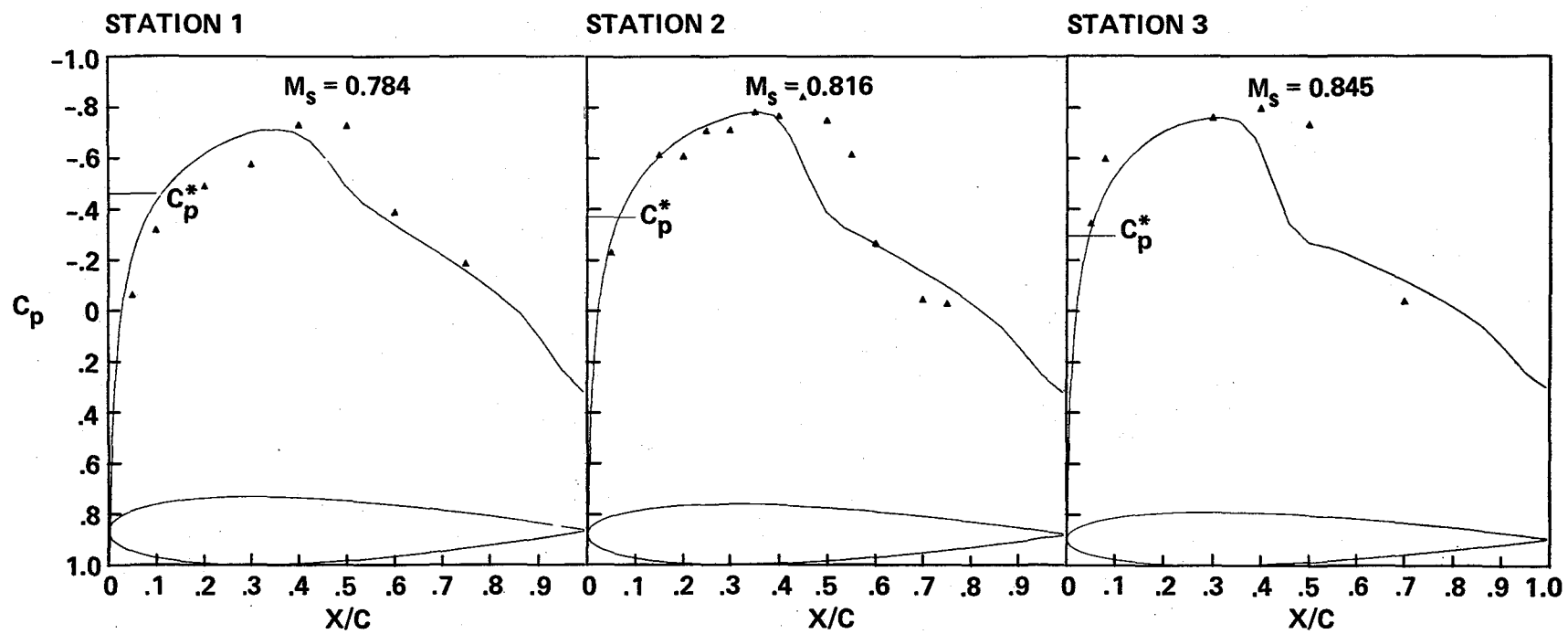
(i)  $\mu = 0.45$ ,  $\psi = 60^\circ$ .

Figure 4.- Continued.



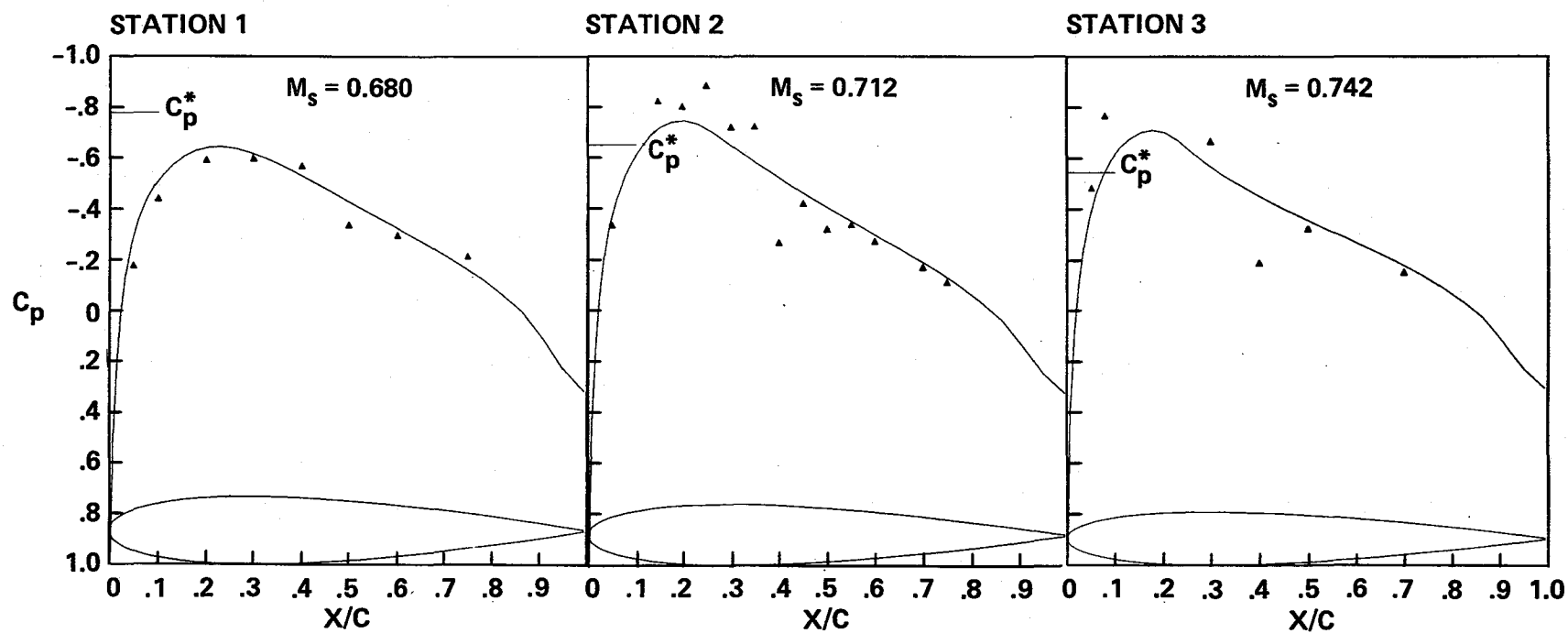
(j)  $\mu = 0.45$ ,  $\psi = 90^\circ$ .

Figure 4.- Continued.



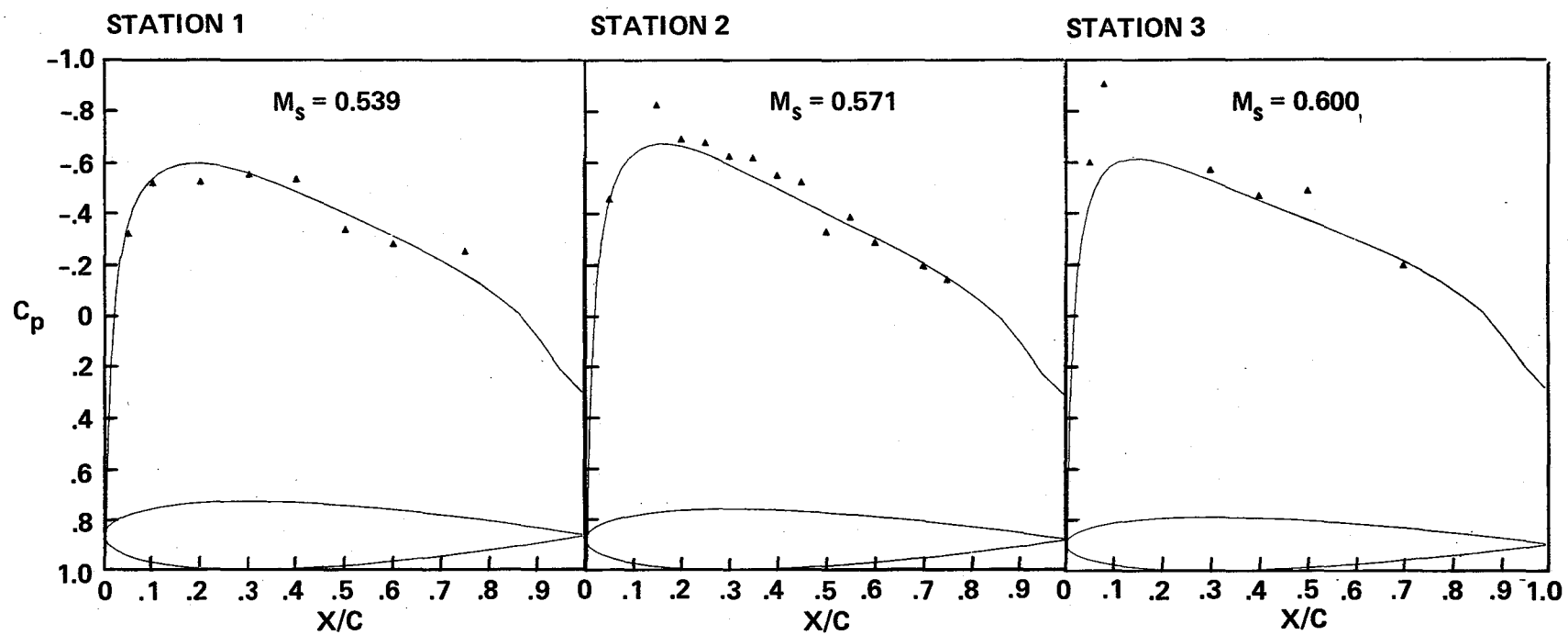
(k)  $\mu = 0.45$ ,  $\psi = 120^\circ$ .

Figure 4.- Continued.



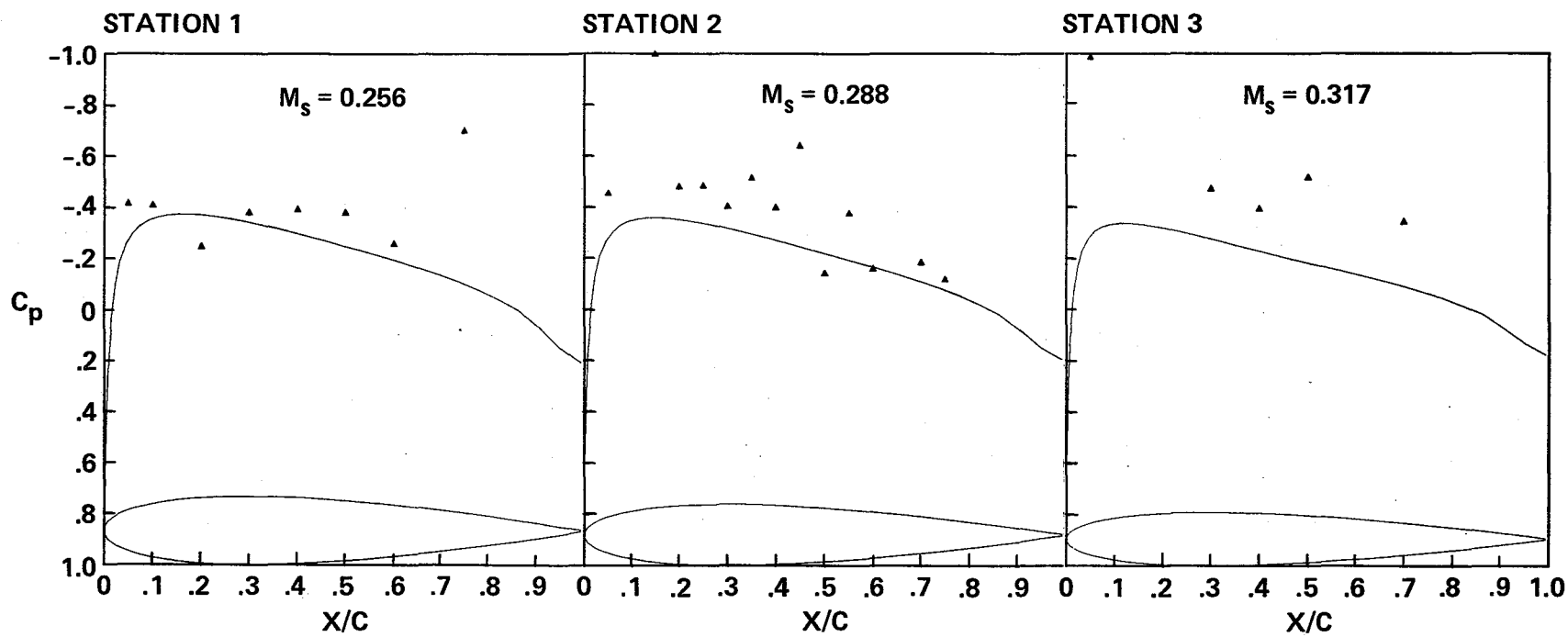
(1)  $\mu = 0.45$ ,  $\psi = 150^\circ$ .

Figure 4.- Continued.



(m)  $\mu = 0.45$ ,  $\psi = 180^\circ$ .

Figure 4.- Continued.



(n)  $\mu = 0.45$ ,  $\psi = 270^\circ$ .

Figure 4.- Concluded.



1. Report No. NASA TM- 85872		2. Government Accession No.		3. Recipient's Catalog No.	
4. Title and Subtitle  COMPARISON OF CALCULATED AND MEASURED PRESSURES ON STRAIGHT- AND SWEEP-TIP MODEL ROTOR BLADES				5. Report Date December 1983	
				6. Performing Organization Code ATP	
7. Author(s) Michael E. Tauber, I-Chung Chang, David A. Caughy,* and Jean-Jacques Philippe <sup>†</sup>				8. Performing Organization Report No. A-9584	
9. Performing Organization Name and Address Ames Research Center, Moffett Field, Calif. 94035 *Cornell University, Ithaca, N.Y. <sup>†</sup> ONERA, Chatillon, France				10. Work Unit No. T-3414Y	
				11. Contract or Grant No.	
12. Sponsoring Agency Name and Address  National Aeronautics and Space Administration Washington, D.C. 20546				13. Type of Report and Period Covered  Technical Memorandum	
				14. Sponsoring Agency Code 505-42-11	
15. Supplementary Notes Point of Contact: Michael Tauber, Ames Research Center, MS 227-8, Moffett Field, Calif. 94035. (415) 965-5656 or FTS 448-5656					
16. Abstract  Using the quasi-steady, full potential code, ROT22, pressures were calculated on straight- and swept-tip model helicopter rotor blades at advance ratios of 0.40 and 0.45, and into the transonic tip speed range. The calculated pressures were compared with values measured in the tip regions of the model blades. Good agreement was found over a wide range of azimuth angles when the shocks on the blade were not too strong. However, strong shocks persisted longer than predicted by ROT22 when the blade was in the second quadrant. Since the unsteady flow effects present at high advance ratios primarily affect shock waves, the underprediction of shock strengths is attributed to the simplifying, quasi-steady, assumption made in ROT22.					
17. Key Words (Suggested by Author(s))  Helicopter rotor aerodynamics			18. Distribution Statement  Unlimited   Subject Category - 02		
19. Security Classif. (of this report) Unclassified		20. Security Classif. (of this page) Unclassified		21. No. of Pages 39	
				22. Price* A03	





